~~Responses~~Reallocation of elemental content and macromolecule ~~of~~in the coccolithophore *Emiliania huxleyi* to ~~reduced phosphorus availability and ocean acidification depend on light intensity~~acclimate to climate change

Yong Zhang[1,*], Yong Zhang[1,§], Shuai Ma[1], Hanbing Chen[2], Jiabing Li[1], Zhengke Li[3], Kui Xu[4], Ruiping Huang[5], Hong Zhang[1], Yonghe Han[1], Jun Sun[6]

[1]College of Environmental and Resource Sciences, College of Carbon Neutral Modern Industry, Fujian Key Laboratory of Pollution Control and Resource Recycling, Fujian Normal University, Fuzhou, China

[2]College of Life Science, Fujian Normal University, Fuzhou, China

[3]School of Food and Biological Engineering, Shanxi University of Science and Technology, Xi'an, China

[4]Hubei Key Laboratory of Edible Wild Plants Conservation and Utilization, Hubei Engineering Research Center of Special Wild Vegetables Breeding and Comprehensive Utilization Technology, College of Life Sciences, Hubei Normal University, Huangshi, China

[5]State Key Laboratory of Marine Environmental Science, College of Ocean and Earth Sciences, Xiamen University, Xiamen, China

[6]Institute for Advanced Marine Research, China University of Geosciences, Guangzhou, China

Running head: Physiology and biochemistry of *E. huxleyi*

*Correspondence: Yong Zhang (yongzhang@fjnu.edu.cn)

Keywords: Carbohydrate; CO_2; coccolithophore; elemental content; light intensity; phosphorus availability; protein.

§Email: qsx20211022@student.fjnu.edu.cn

Abstract

Global climate change leads to simultaneous changes in multiple environmental drivers in the marine realm. Although physiological characterization of coccolithophores have been studied under climate change, there is limited knowledge on the biochemical responses of this biogeochemically important phytoplankton group to changing multiple environmental drivers. Here we investigate the interactive effects of reduced phosphorus availability (4 to 0.4 µmol L^{-1}), elevated pCO_2 concentrations (426 to 946 µatm) and increasing light intensity (40 to 300 µmol photons m^{-2} s^{-1}) on elemental content and macromolecules of the cosmopolitan coccolithophore *Emiliania huxleyi*. Reduced phosphorus availability reduces particulate organic nitrogen and protein contents per cell under 40 µmol photons m^{-2} s^{-1}~~low light intensity~~, but not under 300 µmol photons m^{-2} s^{-1}~~high light intensity~~. Reduced phosphorus availability and~~ ocean acidification~~ elevated pCO_2 concentrations act synergistically to increase particulate organic carbon (POC) and carbohydrate contents per cell under ~~high light intensity~~300 µmol photons m^{-2} s^{-1} but not under ~~low light intensity~~40 µmol photons m^{-2} s^{-1}. Reduced phosphorus availability, ~~ocean acidification~~elevated pCO_2 concentrations and increasing light intensity act synergistically to increase the allocation of POC to carbohydrates. Under ~~future ocean acidification~~elevated pCO_2 concentrations and increasing light intensity, enhanced carbon fixation could increase carbon storage in the phosphorus-limited regions of the oceans where *E. huxleyi* dominates the phytoplankton assemblages. In each light intensity, elemental carbon to phosphorus (C : P) and nitrogen to phosphorus (N : P) ratios decrease with increasing growth rate. These results suggest that coccolithophores could reallocate chemical elements and energy to synthesize macromolecules efficiently, which allows them to regulate its elemental content and

growth rate to acclimate to changing environmental conditions.

1 Introduction

Continuous increase in atmospheric CO_2 level, as a consequence of anthropogenic activities, leads to global and ocean warming, which in turn shoals the ocean upper mixed layer (UML), hinders upward transport of nutrients from deeper ocean to the UML and increases light exposures to phytoplankton cells dwelling therein (Steinacher et al., 2010; Wang et al., 2015). The dissolution of CO_2 in the oceans is causing a significant chemical shift toward higher CO_2 and proton ($[H^+]$) concentrations, a process defined as ocean acidification (OA) (Caldeira and Wickett, 2003). ~~These ocean changes expose phytoplankton cells within the UML to multiple drivers~~Environmental changes in the UML will expose phytoplankton cells to physiological stress, and understanding the effects of changing multiple environmental drivers on the physiology and biochemistry of marine phytoplankton is important for projections of changes in the biogeochemical roles of phytoplankton in the future ocean (Gao et al., 2019).

Coccolithophores take up carbon dioxide (CO_2) to produce particulate organic carbon (POC) via photosynthesis, and use bicarbonate (HCO_3^-) and calcium (Ca^{2+}) to synthesize calcium carbonate plates (coccoliths, PIC) and release CO_2 via calcification, and play a critical role in the marine carbon cycle (Rost and Riebesell, 2004). The cosmopolitan coccolithophore *Emiliania huxleyi* typically forms extensive blooms that are easily detected by satellite remote sensing due to high light scattering caused by coccoliths (Terrats et al., 2020; He et al., 2022). Within *E. huxleyi* blooms in polar and subpolar oceans, dissolved nitrate and phosphate concentrations in surface seawater could be as lower as 0.95 μmol L^{-1} and 0.16 μmol L^{-1}, respectively

(Townsend et al., 1994), light intensity are higher than 300 μmol photons m^{-2} s^{-1} (Tyrrell and Merico, 2004), and the mean concentrations of seawater CO_2 increased by 21.0%–43.3% which weakens the oceanic CO_2 uptake from the atmosphere (Kondrik et al., 2018). *Emiliania huxleyi* is also the dominant phytoplankton species in the lower photic zone in the north-eastern Caribbean Sea (western Atlantic Ocean) (Jordan and Winter, 2000) and in the South Pacific Gyre where dissolved nitrate and phosphate concentration are about 1.0 μmol L^{-1} and 0.2 μmol L^{-1}, respectively, and light intensity is lower than 20 μmol photons m^{-2} s^{-1} (Beaufort et al., 2008; Perrin et al., 2016). In the future ocean, numerous environmental factors will simultaneously change and the extent of these changes may increase (Gao et al., 2019). To explore how *E. huxleyi* acclimate to simultaneous changes in macronutrient concentration, light intensity and CO_2 level, it is interesting to investigate their physiological and biochemical processes, which can also help to project the effect of coccolithophores on ocean carbon cycle and ecological systems.

For more than a decade, research has shown that *E. huxleyi* cells developed several strategies to acclimate to reduced phosphorus availability, increasing light intensity and ocean acidification (Leonardos and Geider, 2005; McKew et al., 2015; Wang et al., 2022). Interactive effects of phosphorus availability and light intensity have shown that under phosphorus limitation condition, cells increased expression and the activity of alkaline phosphatase, and took up and used phosphorus efficiently under high light intensity, whereas they lowered the phosphorus uptake rate under low light intensity (Riegman et al., 2000; Perrin et al., 2016). In addition, the positive effect of reduced phosphorus availability on cellular POC and PIC contents of *E. huxleyi* was further enhanced by increasing light intensity due to high-light-induced increases in CO_2 and HCO_3^- uptake rates under low phosphate availability (Leonardos and Geider,

2005). The negative effect of reduced phosphorus availability on cellular particulate organic phosphorus (POP) content was partly compensated by increased PO_4^{3-} uptake rate under increasing light intensity (Perrin et al., 2016). On the other hand, several studies report that ocean acidification and reduced phosphorus availability acted synergistically to increase the cellular POC content, especially at high light intensity, and acted antagonistically to affect cellular PIC content of *E. huxleyi* (Leonardos and Geider, 2005; Matthiessen et al., 2012; Zhang et al., 2020). In addition, ocean acidification normally amplified the positive effect of increasing light intensity on cellular POC content (Rokitta and Rost, 2012; Heidenreich et al., 2019). Due to high proton concentration-induced reduction in HCO_3^- uptake rate, ocean acidification could weaken or counteract the positive effect of increasing light intensity on cellular PIC content (Rokitta and Rost, 2012; Kottmeier et al., 2016). Overall, while recent studies have focused on physiological performance of *E. huxleyi* and their effects on marine biogeochemical cycling of carbon, little information is available about the biochemical response of *E. huxleyi* to reduced phosphorus availability, increasing light intensity and ocean acidification.

The objective of this study is to investigate the combined effects of reduced phosphorus availability, increasing light intensity and ocean acidification on cellular elemental contents, the carbon (C) : nitrogen (N) : phosphorus (P) ratio and macromolecules of *E. huxleyi*, and to analyze the effects of macromolecules on elemental contents. Under reduced phosphorus availability, increasing light intensity and ocean acidification, we hypothesize that increased cellular POC content is more likely to be caused by increased carbohydrate content. In addition, we discuss the potential mechanisms for changing cellular PIC content in response to changed levels of phosphate, light, and CO_2, which is important for projections of changes in

coccolithophore biogeochemistry and ecology in the future ocean.

2 Materials and Methods

2.1 Experimental setup

Emiliania huxleyi strain RCC1266 (morphotype A) was originally isolated from shelf waters around Ireland (49°30' N, 10°30' W) in 2007 and obtained from the Roscoff algal culture collection (Fig. S1). *Emiliania huxleyi* was cultured under a 14 h : 10 h light : dark cycle (light period: 06:00 to 20:00 h) in a thermo-controlled incubator (MGC-400H, Shanghai Yiheng Scientific Instrument) at 20°C in semicontinuous cultures. The artifical seawater (ASW) media was prepared according to Berges et al. (2001) with a salinity of 33 psu, a boron concentration of 372 μmol L^{-1}, and with the addition of 2350 μmol L^{-1} bicarbonate to achieve the total alkalinity (TA) of 2350 μmol L^{-1}, and enriched with 64 μmol L^{-1} NO_3^-, f/8 concentrations for trace metals and vitamins (Guillard and Ryther, 1962). The experiment was conducted in two parts (Fig. S2~~1~~). The first part (Part 1) was performed at 40 μmol photons m^{-2} s^{-1} (low light intensity, LL) and the second one (Part 2) was at 300 μmol photons m^{-2} s^{-1} (high light intensity, HL). The LL intensity used here corresponds to the lower end of the irradiance range of the UML, and the HL intensity represents to the irradiance in the surface ocean (Jin et al., 2016; Perrin et al., 2016). For each part of the experiment, dissolved inorganic phosphorus (DIP) concentration and ocean acidification were combined in a fully factorial design: high DIP concentration (4 μmol L^{-1})＋low CO_2 level (426 μatm, current CO_2 level) (HP+LC, treatment 1 in LL and treatment 5 in HL), high DIP concentration (4 μmol L^{-1})＋high CO_2 level (946 μatm, future CO_2 level) (HP+HC, treatment 2 in LL and treatment 6 in HL), low DIP concentration (0.43 μmol L^{-1})＋low CO_2 level (426 μatm) (LP+LC, treatment 3 in LL and treatment

7 in HL), and low DIP concentration (0.43 μmol L^{-1})+high CO_2 level (946 μatm) (LP+HC, treatment 4 in LL and treatment 8 in HL). High DIP concentration is replete for physiological process of *E. huxleyi*, and ~~low DIP concentration corresponds to the upper end of the range of phosphate concentration in the coastal waters (Larsen et al., 2004)~~at the end of the incubation, low DIP concentration limits the growth of *E. huxleyi* (see below). There were eight treatments totally and four biological replicates for each treatment (Fig. S2~~1~~). In all cases, cell densities were lower than 78,000 cells mL^{-1} and the cells were acclimated to each treatment for at least 8 generations before physiological and biochemical parameters were measured.

At LL intensity (Part 1), for the treatments of HP+LC and HP+HC, the ASW media were enriched with 4 μmol L^{-1} PO_4^{3-} and aerated for 24 h at 20°C with filter-sterilized (PTFE filter, 0.22 μm pore size, Nantong) air pumped from the room. The pH_{Total} (total scale) values of the media under both HP+LC and HP+HC treatments were about 8.04. The dry air was humidified with Milli-Q water prior to the aeration to minimize evaporation. Under the HP+HC treatment, the pH_{Total} values of the media were adjusted to 7.74 by stepwise additions of CO_2-saturated seawater~~, and the ratio was about 6.5 mL CO_2-saturated seawater : 1000 mL ASW media. The CO_2-saturated seawater was achieved by bubbling pure CO_2 gas into 500 ml ASW media with a total alkalinity of 2350 μmol L^{-1} for 2 h.~~ For the treatments of LP+LC and LP+HC, the ASW media were enriched with 0.4 μmol L^{-1} PO_4^{3-} and aerated for 24 h at 20°C with filtered room air. Under the LP+HC treatment, the pH_{Total} values of the media were also adjusted to 7.74 as described above. The HP+LC, HP+HC, LP+LC and LP+HC seawater were then filtered (0.22 μm pore size, Polycap 75 AS, Whatman) and carefully pumped into autoclaved 50 mL (for TA measurements), 600 mL (for pre-experimental cultures) and 2350 mL (for experimental cultures) polycarbonate

bottles (Nalgene) with no headspace to minimize gas exchange. ~~The volumes of culture inoculum were calculated to match the volumes of media taken out from the bottles prior to inoculation.~~ The cells were inoculated to achieve an initial density of 5000 cells ml^{-1} in the HP+LC and HP+HC conditions, respectively, and cultured for 2 days, then diluted to the initial density again. These processes were performed three times in 600 mL bottles for pre-experimental cultures at 40 μmol photons m^{-2} s^{-1} (LL) of photosynthetically active radiation (PAR; measured using a LI-190SA quantum sensor, Beijing Ligaotai Technology Co. Ltd.). In the main experimental cultures ~~in the HP+LC and HP+HC conditions at LL intensity,~~ the cells were, ~~respectively,~~ transferred from 600 mL to 2350 mL bottles at the same time, and cultured for another 2 days (Fig. S2~~1~~b). Culture bottles were rotated 10 times until cells were mixed at 09:00 h, 13:00 h and 19:00 h. ~~Based on changes in cell densities during the incubations, we calculated that at LL intensity, cells were acclimated to HP+LC and HP+HC conditions for 10 generations.~~ In the second day of the main experimental cultures, subsamples were taken for measurements of cell densities, pH_{Total}, TA, cellular contents of total particulate carbon (TPC), particulate organic carbon (POC), nitrogen (PON) and phosphorus (POP), carbohydrate and protein. At the end of the cultures under the previous conditions, cell samples with an initial density of 5000 cells ml^{-1} were transferred from HP+LC condition (treatment 1) to LP+LC condition (treatment 3), and from HP+HC condition (treatment 2) to LP+HC condition (treatment 4) at LL intensity. The cells were acclimated to LP+LC and LP+HC conditions for 8 generations before subsamples were taken for measurements, which allows cells to have enough time periods to change growth rate against the low DIP concentration.

At HL intensity (Part 2), samples grown under the HP+LC and HP+HC conditions

were transferred from 40 (LL) to 300 μmol photons m^{-2} s^{-1} (HL) of PAR with initial cell density of 5000 cells ml^{-1}. The cells were cultured under the HP+LC and HP+HC conditions for 2 days, respectively, and then diluted back to the initial cell density. These processes were performed three times in 600 mL bottles at HL intensity, and then the main experimental cultures were conducted in 2350 mL bottles. ~~The cells were, respectively, acclimated to HP+LC and HP+HC conditions for at least 8 generations at HL intensity.~~ On the second day of the incubation, subsamples were taken for measurements of the parameters. After that, cell samples with an initial density of 5000 cells ml^{-1} were transferred from HP+LC condition (treatment 5) to LP+LC condition (treatment 7), and from HP+HC condition (treatment 6) to LP+HC condition (treatment 8). At HL intensity, cell samples were acclimated for at least 8 generations in LP+LC and LP+HC conditions, respectively, before subsamples were taken for measurements.

2.2 Phosphate concentration and carbonate chemistry measurements

In the beginning and on the second day of the incubations, samples for determinations of phosphate concentration (20 mL), pH_{Total} value (20 mL) and total alkalinity (TA) (50 mL) were, respectively, filtered (PTFE filter, 0.22 μm pore size, Nantong) 7 h after the onset of the light period (at 13:00). Dissolved inorganic phosphorus (DIP) concentration was measured using a spectrophotometer (SP-722, Shanghai Spectrum Instruments) following the phosphomolybdate method (Hansen and Koroleff, 1999). The bottle for pH measurement was filled from bottom to top with overflow and closed without a headspace. The pH_{Total} value was measured immediately at 20°C using a pH meter which was corrected with a standard buffer of defined pH in seawater (Dickson, 1993). TA samples were treated with 10 μL saturated $HgCl_2$

solution and stored in the dark at 4.0°C, and TA was measured at 20°C by potentiometric titration (AS-ALK1+, Apollo SciTech) according to Dickson et al. (2007). Carbonate chemistry parameters were estimated from TA and pH_{Total} using the CO2SYS program of Pierrot et al. (2006) with carbonic acid constants, K_1 and K_2, taken from Roy et al. (1993).

2.3 Cell density and elemental content measurements

Twenty milliliter samples to monitor the cell density were taken daily at 13:30 h, and fresh media with the same DIP concentration and carbonate chemistry as in the initial treatment conditions were added as top-up. Cell densities were determined using a Multisizer^{TM}3 Coulter Counter (Beckman Coulter). Growth rates were calculated for each replicate according to the equation: $\mu = (\ln N_t - \ln N_0) / d$, where N_t and N_0 refer to the cell densities on the second day and in the beginning of the main experiment, respectively, and d was the growth period in days.

After mixing, samples for determinations of TPC (300 mL), POC and PON (300 mL), and POP (300 mL) were obtained by filtering onto GF/F filters (precombusted at 450°C for 6 h) at the same time (14:00 h) in each treatment. For POC and PON measurements, samples were fumed with HCl for 12 h to remove inorganic carbon. TPC, POC and PON samples were dried at 60°C for 12 h and analyzed using an Elementar CHNS analyzer (Vario EL cube, GmbH, Germany). Cellular particulate inorganic carbon (PIC) content was calculated as the difference between cellular TPC and POC contents (Fabry and Balch, 2010). To remove dissolved inorganic phosphorus from the GF/F filters, POP samples were rinsed three times with 0.17 mol L^{-1} Na_2SO_4. After that, 2 mL 0.017 mol L^{-1} $MgSO_4$ solution was added onto filters, and POP samples were dried at 90°C for 12 h, and then combusted at 500°C for 6 h to

276 remove POC and digested by 0.2 mol L^{-1} HCl (Solórzano and Sharp, 1980).
277 Phosphorus concentration was measured using a microplate reader (Thermo Fisher)
278 following the ammonium molybdate method (Chen et al., 1956) using
279 adenosine-5-triphosphate disodium trihydrate as a standard.
280
281 **2.4 Protein and carbohydrate measurements**
282 Samples for determinations of protein (600 mL) and carbohydrate (600 mL) were,
283 respectively, filtered onto polycarbonate filters (0.6 μm pore size, Nuclepore,
284 Whatman) and onto precombusted GF/F filters at 14:30 h. Protein samples were
285 extracted by bead milling (FastPrep Lysing Matrix D) in 0.5 mL 1 × protein extraction
286 buffer (lithium dodecyl sulfate, ethylene diamine tetraacetic acid, Tris, glycerol and
287 4-(2-aminoethyl) benzenesulfonyl fluoride hydrochloride). Bead milling was
288 performed four times for 1 min at 6.5 ms^{-1}, and samples were placed on ice for 2 min
289 between each round of bead milling to prevent degradation. The samples were then
290 centrifuged at 10,000 × *g* for 5 min (Centrifuge 5418 R, Eppendorf, Germany), and
291 extracted protein in the supernatant was quantified using the BCA assay with bovine
292 gamma globulin as a standard using a microplate reader (Ni et al., 2016).
293 Carbohydrate samples were hydrolyzed with 12.00 mol L^{-1} H_2SO_4 in the dark for 1 h
294 and diluted by Milli-Q water to a final H_2SO_4 concentration of 1.20 mol L^{-1}. Then,
295 samples were sonicated for 5 min, vortexed for 30 s, and boiled at 90°C for 3 h
296 (Pakulski and Benner, 1992). The extracted carbohydrate was determined by phenol
297 sulfuric reaction with D–glucose as standard (Masuko et al., 2005).
298
299 **2.5 Data analysis**
300 The percentages of carbon (C : carbohydrate is 40% and C : protein is 53%) and

nitrogen (N : protein is 16%) contributed by carbohydrate and protein were calculated from the elemental composition of biochemical classes compiled by Geider and LaRoche (2002). A three-way ANOVA was used to determine the main effects of DIP concentration, light intensity and CO_2 level, and their interactions on each variable. A Tukey post hoc test was performed to identify significant differences between two DIP concentrations, two light intensities and two CO_2 levels. A Shapiro–Wilk test was conducted to analyze the normality of residuals and a Levene test was conducted graphically to test for homogeneity of variances. The significant difference between treatments was set at $p < 0.05$. All data analyses were conducted using the statistical software *R* with the packages carData, lattice and nlme (R version 3.5.0).

3 Results

3.1 Dissolved inorganic phosphorus concentration and carbonate chemistry parameters

During the incubations, organismal activity significantly reduces dissolved inorganic phosphorus (DIP) concentrations (Table 1). Under high phosphorus (HP) treatment, DIP concentrations decrease by 20.32% in low light (LL) and low CO_2 (LC), by 22.32% in LL and high CO_2 (HC), by 27.66% in high light (HL) and LC, and by 31.58% in HL and HC. Under low phosphorus (LP) treatment, DIP concentrations decrease from 0.43 μmol L^{-1} at the beginning of the experiment to be lower than 0.04 μmol L^{-1} (the detection limit) at the end of the incubation in LL and LC conditions, in LL and HC conditions, in HL and LC conditions, and in HL and HC conditions.

During the incubations, at LL intensity, pH_T values increase by, on average, 0.02 in HP+LC, by 0.03 in HP+HC, by 0.09 in LP+LC, and by 0.10 in LP+HC conditions (Table 1). At HL intensity, pH_T values increase by 0.05 in HP+LC, by 0.06 in HP+HC,

by 0.12 in LP+LC, and by 0.09 in LP+HC conditions. Correspondingly, at LL intensity, seawater CO_2 concentrations decrease by 5.53% in HP+LC, by 6.89% in HP+HC, by 22.76% in LP+LC, and by 22.77% in LP+HC. At HL intensity, seawater CO_2 concentrations decrease by 16.18% in HP+LC, by 16.41% in HP+HC, by 28.92% in LP+LC, and by 22.30% in LP+HC. Overall, organismal activity has larger effects on carbonate chemistry under the LP treatment than under the HP treatment.

3.2 Growth rate

The effect of increasing light intensity on growth rate is positive which can be seen by comparing growth rate in the HL regimes with their paired LL regimes (Fig. 1a~~,b~~; Table 2), though the extent of increase in growth rate depends on CO_2 levels and phosphate availability. Compared to LL intensity, growth rates at HL intensity increased by 48.48% in HP+LC, by 50.87% in HP+HC, by 60.86% in LP+LC, and by 60.80% in LP+HC (Tukey post hoc test, all values of $p < 0.01$). The effect of increasing CO_2 levels on growth rate depends on light intensity and phosphate availability (Fig. 1a~~,b~~). Compared to LC level, growth rates in HC level decreased by 3.08% in LL and HP condition ($p = 0.48$), by 16.13% in LL and LP condition ($p < 0.01$), by 1.50% in HL and HP condition ($p = 0.68$), and by 16.27% in HL and LP condition ($p < 0.01$). The effect of reduced phosphorus availability on growth rate is negative and the extent of reduction in growth rate depends on light intensity and CO_2 levels (Fig. 1a~~,b~~). Compared to HP availability, growth rates in LP availability decreased by 8.46% in LL and LC condition ($p <0.01$), by 20.81% in LL and HC condition ($p < 0.01$),~~ by 0.76% in HL and LC condition ($p = 0.99$),~~ and by 15.63% in HL and HC condition ($p < 0.01$)<u>, and did not change significantly in HL and LC condition ($p = 0.99$)</u>. These results show that high CO_2 levels and low phosphorus

availability acted synergistically to reduce growth rate of *E. huxleyi*, and increasing light intensity could partly counteract this response (Table S1).

3.3 Cellular POC, PON, POP and PIC contents

The effect of increasing light intensity on cellular POC content is positive, which was observed by comparing POC content in all the HL regimes with their paired LL regimes (Fig. 1b~~c,d~~). The extent of increase in POC content depends on CO_2 levels and phosphate availability. Compared to LL intensity, cellular POC contents at HL intensity increased by 27.15% in HP+LC, by 26.51% in HP+HC, by 43.24% in LP+LC, and by 58.13% in LP+HC conditions (Tukey post hoc test, all values of $p < 0.01$). The effect of increasing CO_2 levels on POC content is light and phosphate dependent and can be seen by comparing POC content in the HC regimes with their paired LC regimes (Fig. 1b~~c,d~~). At LL intensity, cellular POC contents are not significantly different between HP+LC, HP+HC, LP+LC and LP+HC conditions (all values of $p > 0.1$). At HL intensity, compared to LC level, cellular POC contents in HC level increased by 5.12% in HP condition ($p = 0.74$), and by 8.28% in LP condition ($p = 0.07$). The effect of phosphate reduction on POC content is light and CO_2 dependent, which can be seen by comparing POC content in the LP regimes with those in their paired HP regimes (Fig. 1b~~c,d~~). At LL intensity, cellular POC contents did not significantly differ between LP and HP availability. At HL intensity, compared to HP availability, cellular POC contents in LP availability increased by 11.80% in LC condition ($p = 0.02$), and by 15.28% in HC condition ($p < 0.01$). These results show that ocean acidification and reduced phosphorus availability acted synergistically to increase POC contents in HL condition but not in LL condition (Table S1).

The effect of increasing light intensity on cellular PON content depends on CO_2 levels and phosphate availability (Fig. 1c~~e,f~~). Compared to LL intensity, cellular PON contents at HL intensity increased by 12.03% in HP+LC condition (p = 0.27), by 19.54% in HP+HC condition (p < 0.01), by 22.68% in LP+LC condition (p < 0.01), and by 30.90% in LP+HC condition (p < 0.01). The effect of increasing CO_2 levels on PON content is light and phosphate dependent, which can be seen by comparing POC content in the HC regimes with their paired LC regimes (Fig. 1c~~e,f~~). Compared to LC level, cellular PON contents in HC level did not change significantly in LL and HP condition, in LL and LP condition, in HL and LP condition, and increased by 14.68% in HL and HP condition (p = 0.02). The effect of phosphate reduction on PON content is CO_2 and light dependent, which can be seen by comparing PON content in the LP regimes with those in their paired HP regimes (Fig. 1c~~e,f~~). Compared to HP availability, cellular PON contents in LP availability decreased by 16.59% in LL and LC condition (p = 0.01), by 24.03% in LL and HC condition (p < 0.01), by 8.35% in HL and LC condition (p = 0.43), and by 17.32% in HL and HC condition (p < 0.01). These results show that increasing light intensity compensated for the negative effect of phosphate reduction on PON content (Table S1).

The effect of increasing light intensity on POP content is positive and can be seen by comparing POP content in the HL regimes with their paired LL regimes, though the extent of increase in POP content depends on CO_2 levels and phosphate availability (Fig. 1d~~g,h~~). Compared to LL intensity, cellular POP contents at HL intensity increased by 35.79% in HP+LC, by 41.70% in HP+HC, by 57.22% in LP+LC, and by 56.44% in LP+HC conditions (Tukey post hoc test, all values of p < 0.01). Ocean acidification did not change the POP contents significantly ~~in LL and HP condition, in LL and LP condition, in HL and HP condition, and in HL and LP~~

~~condition~~ under all treatments used here (all values of $p > 0.53$) (Fig. 1~~dg,h~~). Reduced phosphorus availability significantly decreased the POP contents, which can be seen by comparing POP content in the LP regimes with their paired HP regimes, though the extent of reduction in POP content depends on light intensity and CO_2 levels (Fig. 1~~dg,h~~). Compared to HP availability, cellular POP contents in LP availability decreased by 52.96% in LL and LC condition, by 54.03% in LL and HC condition, by 46.11% in HL and LC condition, and by 49.51% in HL and HC condition (all values of $p < 0.01$). These results show that reduced phosphorus availability had a larger effect on POP content than that of ocean acidification and increasing light intensity (Table S1).

The effect of increasing light intensity on PIC content is positive, which can be seen by comparing PIC content in the HL regimes with their paired LL regimes, though the extent of increase in PIC content depends on CO_2 levels and phosphorus availability (Fig. 1~~ei,j~~). Compared to LL intensity, cellular PIC contents at HL intensity increased by 77.87% in HP+LC, by 70.28% in HP+HC, by 98.31% in LP+LC, and by 90.68% in LP+HC conditions (Tukey post hoc test, all values of $p < 0.01$). The effect of increasing CO_2 levels on PIC content is negative and can be seen by comparing PIC content in the HC regimes with those in their paired LC regimes (Fig. 1~~ei,j~~). The extent of reduction in PIC content depends on light intensity and phosphorus availability. Compared to LC level, cellular PIC contents under ocean acidification decreased by 31.43% in LL and HP condition ($p = 0.09$), by 16.00% in LL and LP condition ($p = 0.67$), by 35.02% in HL and HP condition ($p < 0.01$), and by 21.12% in HL and LP condition ($p < 0.01$). The effect of phosphate reduction on PIC content is positive which can be seen by comparing PIC content in the LP regimes with their paired HP regimes, though the extent of increase in PIC content

depends on light intensity and CO_2 levels (Fig. 1e~~i,j~~). Compared to HP availability, cellular PIC contents in LP availability increased by 16.00% in LL and LC condition (p = 0.83), by 41.26% in LL and HC condition (p = 0.16), by 29.98% in HL and LC condition (p < 0.01), and by 60.44% in HL and HC condition (p < 0.01). These results show that high light intensity and low phosphorus availability acted synergistically to increase PIC content, which counteracts the negative effect of ocean acidification on PIC content (Table S1).

3.4 Carbohydrate and protein contents

The effect of increasing light intensity on carbohydrate content is positive and can be seen by comparing carbohydrate content in the HL regimes with their paired LL regimes, though the extent of increase in carbohydrate depends on CO_2 levels and phosphorus availability (Fig. 2a~~,b~~). Compared to LL intensity, cellular carbohydrate contents at HL intensity increased by 148.81% in HP+LC condition, by 139.42% in HP+HC condition, by 179.12% in LP+LC condition, and by 204.42% in LP+HC condition (all values of p < 0.01). The effect of increasing CO_2 levels on carbohydrate content is light and phosphate dependent which can be seen by comparing carbohydrate content in the HC regimes with their paired LC regimes (Fig. 2a~~,b~~). Compared to LC level, cellular carbohydrate contents under ocean acidification did not change significantly under LL condition, and increased ~~by 26.55% in LL and HP condition (p = 0.58), by 8.91% in LL and LP condition (p = 0.99),~~ by 21.32% in HL and HP condition (p = 0.02), and by 18.45% in HL and LP condition (p < 0.01). The effect of phosphate reduction on carbohydrate content is light and CO_2 dependent and can be seen by comparing carbohydrate content in the LP regimes with their paired HP regimes (Fig. 2a~~,b~~). Compared to HP availability, cellular carbohydrate contents

in LP availability did not change significantly in LL and LC condition, in LL and HC condition (both $p > 0.65$) and increased by 40.13% in HL and LC condition ($p < 0.01$), and by 36.00% in HL and HC condition ($p < 0.01$). These results show that increasing light intensity dominantly increased carbohydrate content, and ocean acidification and reduced phosphorus availability acted synergistically to increase carbohydrate contents under high light intensity (Table S1).

The effect of increasing light intensity on cellular protein content is positive, which can be seen by comparing protein content in the HL regimes with their paired LL regimes, though the extent of increase in protein content depends on CO_2 level and phosphorus availability (Fig. 2b~~c,d~~). Compared to LL intensity, cellular protein contents at HL intensity increased by 24.76% in HP+LC condition, by 30.43% in HP+HC condition, by 68.09% in LP+LC condition, and by 65.39% in LP+HC condition (all values of $p < 0.01$). The effect of increasing CO_2 levels on protein content can be seen by comparing protein content in the HC regimes with their paired LC regimes (Fig. 2b~~c,d~~). Compared to LC level, cellular protein contents under ocean acidification did not change significantly in LL and HP condition, in LL and LP condition, in HL and HP condition, and in HL and LP condition (all values of $p > 0.09$). The effect of phosphate reduction on protein content is light and CO_2 dependent, which can be seen by comparing protein content in the LP regimes with their paired HP regimes (Fig. 2b~~c,d~~). Compared to HP availability, cellular protein content in LP availability decreased by 27.88% in LL and LC condition, by 28.80% in LL and HC condition (both $p < 0.01$) and did not change significantly in HL and LC condition, and in HL and HC condition (both $p > 0.11$). These results show that high light intensity counteracted the negative effect of low phosphorus availability on protein content, and ocean acidification had less effect on protein content (Table S1).

3.5 Percentage of POC allocated to carbohydrate (carbohydrate–C : POC) and protein (protein–C : POC)

Increasing light intensity increased the percentage of POC allocated to carbohydrate (carbohydrate–C : POC), which can be seen by comparing carbohydrate–C : POC in the HL regimes with their paired LL regimes, though the extent of increase in carbohydrate–C : POC depends on CO_2 levels and phosphorus availability (Fig. 2ce,f). Compared to LL intensity, carbohydrate–C : POC at HL intensity increased by 95.60% in HP+LC condition, by 97.69% in HP+HC condition, by 95.05% in LP+LC condition, and by 83.37% in LP+HC condition (all values of $p < 0.01$). The effect of increasing CO_2 levels on carbohydrate–C : POC is light and phosphate dependent, and can be seen by comparing carbohydrate–C : POC in the HC regimes with their paired LC regimes (Fig. 2ce,f). Compared to LC level, carbohydrate–C : POC under ocean acidification increased by 20.12% in LL and HP condition, by 11.42% in LL and LP condition, by 20.36% in HL and HP condition, and by 4.40% in HL and LP condition (all values of $p > 0.08$). The effect of phosphate reduction on carbohydrate–C : POC is light and CO_2 dependent, which can be seen by comparing carbohydrate–C : POC in the LP regimes with those in their paired HP regimes (Fig. 2ce,f). Compared to HP availability, carbohydrate–C : POC in LP availability increased by 25.61% in LL and LC condition ($p = 0.16$), by 17.37% in LL and HC condition ($p = 0.47$), by 25.81% in HL and LC condition ($p < 0.01$), and by 8.11% in HL and HC condition ($p < 0.05$). These results show that increasing light intensity, ocean acidification and reduced phosphorus availability acted synergistically to increase the percentage of POC allocated to carbohydrate (Table S1).

Increasing light intensity did not significantly change the percentage of POC

allocated to protein (protein–C : POC) ~~in HP+LC, HP+HC, LP+LC and LP+HC conditions~~under the phosphorus availability and CO_2 levels used here (Fig. 2~~dg,h~~). Ocean acidification did not significantly affect the protein–C : POC in LL and HP, in LL and LP, in HL and HP, and in HL and LP conditions. The effect of phosphate reduction on protein–C : POC is light and CO_2 dependent, which can be seen by comparing the protein–C : POC in the LP regimes with their paired HP regimes (Fig. 2~~dg,h~~). Compared to HP availability, protein–C : POC in LP availability decreased by 27.39% in LL and LC condition ($p < 0.01$), by 23.05% in LL and HC condition ($p < 0.01$), by 12.81% in HL and LC condition ($p = 0.09$), and by 21.77% in HL and HC condition ($p < 0.01$). These results show that reduced phosphorus availability dominantly reduced the protein–C : POC, and increasing light intensity and ocean acidification had less effects on protein–C : POC (Table S1). On the other hand, increasing light intensity, reduced phosphorus availability and ocean acidification did not significantly change the percentage of PON allocated to protein (protein–N : PON) (Fig. 2e).

3.6 Elemental stoichiometry and protein content as a function of growth rate

Reduced phosphorus availability increased the POC : PON ratio, and the extent of the increase was larger under HL than LL intensity (Fig. S5a). At LL and HL intensities, both POC : POP ratio and PON : POP ratio were linearly and negatively correlated with growth rates (Fig. 3a,b). In LL and HL conditions, POC : POP ratio decreased linearly with increasing growth rate ($R^2 = 0.71$, $F = 32.08$, $p < 0.01$ in LL condition; $R^2 = 0.53$, $F = 14.63$, $p < 0.01$ in HL condition). Similarly, in LL and HL conditions, PON : POP ratio decreased linearly with increasing growth rate ($R^2 = 0.69$, $F = 29.23$, $p < 0.01$ in LL condition; $R^2 = 0.50$, $F = 13.31$, $p < 0.01$ in HL condition). In all

526 treatments, protein content increased linearly with increasing growth rate (R^2 = 0.76,
527 F = 151.14, p < 0.01) (Fig. 3c), and POC content increased linearly with increasing
528 carbohydrate content (R^2 = 0.94, F = 435.10, p < 0.01) (Fig. 3d).
529
530 **4 Discussion**
531 Coccolithophores ~~make an important contribution to marine biological carbon~~
532 ~~pump~~play a complex role in the marine carbon cycle through production and export of
533 organic carbon to depth but also through the carbonate counter pump, and their
534 responses to global climate change could have significant consequences for marine
535 carbon cycling (Riebesell et al., 2017). The bloom-forming coccolithophore *E. huxleyi*,
536 dominating the assemblages in seawater under limited phosphorus condition, is likely
537 to be exposed to increasing light intensity and ocean acidification in the future ocean
538 (Kubryakova et al., 2021). In this study, we observed that increasing light intensity
539 compensates for the negative effects of low phosphorus availability on cellular protein
540 and nitrogen contents (Figs. 1 and 2). Reduced phosphorus availability, increasing
541 light intensity and ocean acidification act synergistically to increase cellular contents
542 of carbohydrate and POC, and the allocation of POC to carbohydrate. These
543 ~~regulation mechanisms~~changes in *E. huxleyi* could provide vital information for
544 evaluating carbon cycle in marine ecosystems under global change.
545 Ribonucleic acid (RNA) is the main phosphorus-containing macromolecule within
546 the cell (Geider and La Roche, 2002). Therefore, the reduced phosphorus availability
547 dominantly reduces the RNA content (Fig. S6~~5~~), which contributes to low POP
548 contents (McKew et al., 2015) (Fig. 1d~~g,h~~). In eukaryotic cells, ribosomal RNA
549 (rRNA) constitutes about 80% of the total RNA and is mainly used to create ribosome
550 (Dyhrman, 2016). Thus, reduced RNA contents decrease the numbers of ribosome,

which has a potential to decrease protein synthesis (Dyhrman, 2016; Rokitta et al., 2016). On the other hand, the separation of the regression line between POC : POP ratio (or PON : POP ratio) and growth rate under low and high light intensities suggests different POP storage contents in *E. huxleyi* among different light intensities (Perrin et al., 2016).~~On the other hand,~~ ~~l~~Low light intensity down-regulates the expression of genes related to nitrate reductase and nitrite reductase, and then reduces the nitrate uptake and assimilation efficiency of *E. huxleyi* and other phytoplankton species (Perrin et al., 2016; Lu et al., 2018), which exacerbates the negative effect of low phosphorus availability on protein synthesis and PON contents (Figs. 1c~~e~~ and 2b~~e~~). Besides that, low light intensity significantly reduces the rates of RNA synthesis, carbohydrate synthesis and cell division (Zhang et al., 2021), which adds to the negative effect of low phosphorus availability on growth rate of *E. huxleyi* (Fig. 1a). Under high light intensity and low CO_2 level, reduced phosphorus availability did not change growth rate and protein content (Figs. 1a~~b~~ and 2b~~d~~), which suggests that *E. huxleyi* might compensate for low phosphate-induced decreases in ribosome content by increasing protein synthesis efficiency under increasing light intensity (Reith and Cattolico, 1985). Under high light intensity and ocean acidification, reduced phosphorus availability did not significantly change cellular protein content while reduced growth rate, which might indicate the lowered protein synthesis efficiency (McKew et al., 2015).

Several studies report that reduced phosphorus availability (0.4–0.5 μmol L^{-1}) did not change growth rates significantly during the short-time (2 or 3 days) incubations under low CO_2 level and high light intensity (Rokitta et al., 2016; Zhang et al., 2020; Wang et al., 2022) ~~(Fig. S6)~~. The reasons could be that *E. huxleyi* cells developed high affinity for phosphate and increased the uptake rate of phosphate (Wang et al.,

2022) and could replace the phospholipid membrane with non-phosphorus membrane during the short-time incubation of phosphorus limitation (Shemi et al., 2016). Our data showed that reduced phosphorus availability and ocean acidification acted synergistically to reduce growth rate under both low and high light intensities (Fig. 1a~~,b~~). One of the reasons could be that low pH value under ocean acidification up regulates the expressions of a series of genes involved in ribosome metabolism, such as genes of large subunit ribosomal protein L3, L38E, L30E (*RP-L3*, *RP-L38E*, *RP-L30E*), and small subunit ribosomal protein S3E, S5E, SAE (*PR-S3E*, *PR-S5E*, *RP-SAE*) in *E. huxleyi* (Wilson and Doudna Cate, 2012) (Fig. S7). Under ocean acidification, up regulation of expression of these genes has the potential to drive cells to allocate more phosphorus to synthesize ribosome, and to reduce the allocation of phosphorus to DNA replication (Rokitta et al., 2011), which exacerbates the limitation of reduced phosphorus availability on the rate of cell division in *E. huxleyi* (Rouco et al., 2013). Under phosphorus-replete condition, more phosphorus is reallocated to ribosome metabolism under ocean acidification which could facilitate nitrogen assimilation (Fig. 2b~~d~~). Overall, under high light intensity, ocean acidification is likely to facilitate *E. huxleyi* cells to increase nitrogen content in phosphorus-replete condition and to reduce growth rate in phosphorus-limitation.

In this study, we found that low light intensity dominantly limits carbon assimilation of *E. huxleyi* and reduces the effects of phosphate availability and ocean acidification on cellular carbohydrate and POC contents (Figs. 1b~~c~~ and 2a). However, under high light intensity, *E. huxleyi* had high carbohydrate and POC contents while low growth rate under reduced phosphorus availability and ocean acidification (Figs. 1a,b~~b,d~~ and 2a~~b~~), which suggests that carbon assimilation rate did not change significantly while cell division rate decreased (Matthiessen et al., 2012; Perrin et al.,

2016). Furthermore, carbohydrate is a carbon- and energy-storing macromolecule, and protein is related to growth rate (Geider and La Roche, 2002). Under high light intensity, reduced phosphorus availability and ocean acidification, *E. huxleyi* cells could synthesize more carbohydrate to store carbon and energy but didn't increase protein content, which contributes to the large percentage of POC allocated to carbohydrate (Fig. 2c~~f~~).

The physiological reasons for reduced calcification rate under ocean acidification could be due to high proton concentration-induced reduction in HCO_3^- uptake rate (Meyer and Riebesell, 2015; Kottmeier et al., 2016). The molecular mechanisms for low PIC content under ocean acidification may be due to down-regulation of a series of genes potentially involved in ion transport and pH regulation, such as genes of calcium/proton exchanger (*CAX3*), sodium/proton exchanger (*NhaA2*) and membrane-associated proton pump (*PATP*) (Mackinder et al., 2011; Lohbeck et al., 2014). On the other hand, increasing light intensity up-regulates a series of genes related to ion transport, such as gene of *CAX3*, gene of Cl^-/HCO_3^- exchanger and genes of various subunits of a vacuolar H^+–ATPase (*V–ATPase*) and so on (Rokitta et al., 2011). Up-regulation of these genes in high light intensity has the potential to facilitate cells to take up HCO_3^- and Ca^{2+}, and to pump proton outside the cells, and then leads to large PIC content of *E. huxleyi* (Kottmeier et al., 2016). Our data suggest that increasing light intensity counteracts the negative effect of ocean acidification on cellular PIC content of *E. huxleyi* (Fig. 1e~~i,j~~). These results are consistent with the findings of Feng et al. (2020) who reported that combinations of increasing light intensity and ocean acidification increase the expression of genes involved in calcium-binding proteins (*CAM* and *GPA*), which has the potential to increase calcium influx into cells and then compensate for the effect of reduced HCO_3^- uptake

626 rate on calcification. It is also suggested that increasing light intensity could cause
627 cells to remove H^+ faster which neutralizes the effect of high proton concentration on
628 calcification (Jin et al., 2017). On the other hand, reduced phosphorus availability
629 extends the G1 phase of cell cycle where calcification occurs, which prolongs the
630 calcification time and then increases cellular PIC content (Müller et al., 2008). In
631 addition, reduced phosphorus availability up-regulates expressions of genes of Ca^{2+}
632 uptake, proton removal and carbonic anhydrase, and then increases coccolith
633 production (Wang et al., 2022), which contribute to a larger PIC content and
634 counteract the negative effect of ocean acidification on PIC contents (Borchard et al.,
635 2011) (Fig. 1e~~i,j~~). Furthermore, one of the reasons for larger PIC contents under
636 reduced phosphorus availability and increasing light intensity conditions are likely
637 due to larger and more numerous coccoliths (Gibbs et al., 2013; Perrin et al., 2016).
638 Overall, responses of calcification of *E. huxleyi* to ocean climate change are complex
639 than previously thought (Meyer and Riebesell, 2015), and it is worth exploring the
640 underlying mechanisms of calcification under changing multiple environmental
641 drivers (Mackinder et al., 2011; Feng et al., 2020).

642 Cellular POP content of *E. huxleyi* generally decreased, and POC : POP ratio and
643 PON : POP ratio increased with reducing phosphorus availability (Leonardo and
644 Geider, 2005; McKew et al., 2015). The negative correlations between growth rate
645 and POC : POP ratio or PON : POP ratio under each light intensity are consistent with
646 the growth rate hypothesis (Fig. 3), which proposes that growth rate increases with
647 increasing RNA : protein ratio. Phosphorus in RNA accounts for a high percentage of
648 total POP, whereas nitrogen in protein is the main form of PON (Zhang et al., 2021),
649 and the growth rate hypothesis suggests that growth rate could increase with
650 decreasing POC : POP ratio or PON : POP ratio (Sterner and Elser, 2002). Our results

suggest that *E. huxleyi* could reallocate chemical elements and energy to synthesize carbohydrate, protein and RNA efficiently, and then regulate its elemental stoichiometry and growth rate to acclimate to reduced phosphorus availability, ocean acidification and increasing light intensity (Moreno and Martiny, 2018).

In the future ocean, large carbohydrate and POC contents, POC : PON ratio, and POC : POP ratio of coccolithophores indicate increases in carbon export to the deep ocean that may affect the efficiency of the biological carbon pump and the marine biogeochemical cycle of carbon (Meyer and Riebesell, 2015). In addition, increased cellular PIC content under phosphorus limitation condition may have the potential to weaken CO_2 uptake of the oceans in phosphorus-limited marine environments. In summary, responses of coccolithophores to climate change is likely to affect the marine carbon cycle in the future (Riebesell et al., 2017).

Data availability. The data are available upon request to the corresponding author (yongzhang@fjnu.edu.cn).

Author contributions. YZ (yongzhang@fjnu.edu.cn), ZL and KX contributed to the design of the experiment. YZ (yongzhang@fjnu.edu.cn), YZ (qsx20211022@student.fjnu.edu.cn), SM, HC and RH performed this experiment and biochemical analyses. YZ (yongzhang@fjnu.edu.cn) wrote the first manuscript draft. All authors contributed to the data analyses and editing of the paper.

Competing interests. The authors declare that they have no conflict of interest.

Acknowledgments. We would like to thank Professor Zoe V. Finkel for providing the *Emiliania huxleyi* RCC1266, Dr. Vinitha Ebenezer for her helpful revision of the manuscript, and Dr. Peng Jin and two anonymous reviewers for their helpful suggestions which have help us to improve the manuscript. This work was supported by the National Natural Science Foundation of China (41806129 [YZ], 32001180 [ZKL]).

References

Beaufort, L., Couapel, M., Buchet, N., Claustre, H., and Goyet, C.: Calcite production by coccolithophores in the southeast Pacific Ocean, Biogeosciences, 5, 1101–1117, doi:10.5194/bg-5-1101-2008, 2008.

Berges, J. A., Franklin, D. J., and Harrison, P. J.: Evolution of an artificial seawater medium: improvements in enriched seawater, artificial water over the past two decades, J. Phycol., 37, 1138–1145, doi: 10.1046/j.1529-8817.2001.01052.x, 2001.

Borchard, C., Borges, A. V., Händel, N., and Engel, A.: Biogeochemical response of *Emiliania huxleyi* (PML B92/11) to elevated CO_2 and temperature under phosphorus limitation: A chemostat study, J. Exp. Mar. Biol. Ecol., 410, 61–71, doi: 10.1016/j.jembe.2011.10.004, 2011.

Caldeira, K., and Wickett, M. E.: Oceanography: anthropogenic carbon and ocean pH, Nature, 425, 365, doi: 10.1038/425365a, 2003.

Chen, P., Toribara, T. T., and Warner, H.: Microdetermination of phosphorus, Anal. Chem., 28, 1756–1758, doi: 10.1021/ac60068a036, 1956.

Dickson, A. G., Sabine, C. L., and Christian, J. R.: Guide to best practice for ocean CO_2 measurements, PICES Special Publication 3, pp. 191, 2007.

Dickson, A. G.: pH buffers for seawater media based on the total hydrogen ion concentration scale, Deep-Sea Res., 40, 107–118, doi: 10.1016/0967-0637(93)90055-8, 1993.

Dyhrman, S. T.: Nutrients and their acquisition: phosphorus physiology in microalgae, in: The physiology of microalgae, edited by: Borowitzka, M. A., Beardall, J. and Raven, J. A., Springer, Heidelberg, 155–183, doi: 10.1007/978-3-319-24945-2, 2016.

726 Fabry, V. J., and Balch, W. M.: Direct measurements of calcification rates in
727 planktonic organisms, in: Guide to best practices for ocean acidification research
728 and data reporting, edited by: Riebesell, U., Fabry, V. J., Hansson, L. and
729 Gattuso, J. P., Luxembourg, Publications Office of the European Union, p. 201–
730 212, doi: 10.2777/66906, 2010.
731 Feng, Y. Y., Roleda, M. Y., Armstrong, E., Summerfield, T. C., Law, C. S., Hurd, C.
732 L., and Boyd, P. W.: Effects of multiple drivers of ocean global change on the
733 physiology and functional gene expression of the coccolithophore *Emiliania*
734 *huxleyi*, Glob. Chang. Biol., 26, 5630–5645, doi: 10.1111/GCB.15259, 2020.
735 Gao, K., Beardall, J., Häder, D. P., Hall-Spencer, J. M., Gao, G., and Hutchins, D. A.:
736 Effects of ocean acidification on marine photosynthetic organisms under the
737 concurrent influences of warming, UV radiation, and deoxygenation, Front. Mar.
738 Sci., 6, 322, https://doi.org/10.3389/fmars.2019.00322, 2019.
739 Geider, R. J., and LaRoche, J.: Redfield revisited: variability of C:N:P in marine
740 microalgae and its biochemical basis, Eur. J. Phycol., 37, 1–17, doi:
741 10.1017/S0967026201003456, 2002.
742 Gibbs, S. J., Poulton, A. J., Brown, P. R., Daniels, C. J., Hopkins, J., Young, J. R.,
743 Jones, H. L., Thiemann, G. J., O'Dea, S. A., and Newsam, C.: Species-specific
744 growth response of coccolithophores to Palaeocene−Eocene environmental
745 change, Nat. Geosci., 6, 218–222, doi: 10.1038/ngeo1719, 2013.
746 Guillard, R. R. L., and Ryther, J. H.: Studies of marine planktonic diatoms. I.
747 Cyclotella nana Hustedt and Detonula confervacea Cleve, Can. J. Microbiol., 8,
748 229–239, doi: 10.1139/m62-029, 1962.
749 Hansen, H. P., and Koroleff, F.: Determination of nutrients, in: Methods of seawater
750 analysis, edited by: Grasshoff, K., Kremling, K. and Ehrhardt, M., WILEY-VCH

751 Publishers, ISBN: 3-527-29589-5, 1999.
752 He, S., Le, C., He, J., and Liu, N.: Empirical algorithm for detecting coccolithophore
753 blooms through satellite observation in the Barents Sea, Remote Sens. Environ.,
754 270, 112886, doi: 10.1016/j.res.2021.112886, 2022.
755 Heidenreich, E., Wördenweber, R., Kirschhöfer, F., Nusser, M., Friedrich, F., Fahl, K.,
756 Kruse, O., Rost, B., Franzreb, M., Brenner-Weiß, G., and Rokitta, S.: Ocean
757 acidification has little effect on the biochemical composition of the
758 coccolithophore *Emiliania huxleyi*, PLoS One, 14, e0218564, doi:
759 10.1371/journal.pone.0218564, 2019.
760 Jin, P., Gao, G., Liu, X., Li, F., Tong, S., Ding, J., Zhong, Z., Liu,N., and Gao, K.:
761 Contrasting photophysiological characteristics of phytoplankton assemblages in
762 the Northern South China Sea, PLoS ONE, 11, e0153555, doi:
763 10.1371/journal.pone.0153555, 2016.
764 Jin, P., Ding, J. C., Xing, T., Riebesell, U., and Gao, K. S.: High levels of solar
765 radiation offset impacts of ocean acidification on calcifying and non-calcifying
766 strains of *Emiliania huxleyi*, Mar. Ecol. Prog. Ser., 568, 47–58, doi:
767 10.3354/meps12042, 2017.
768 Jordan, R. W., and Winter, A: Assemblages of coccolithophorids and other living
769 microplankton off the coast of Puerto Rico during January–May 1995, Mar.
770 Micropaleontol., 39, 113–130, doi: 10.1016/S0377-8398(00)00017-7, 2000.
771 Kondrik, D. V., Pozdnyakov, D. V., and Johannessen, O. M.: Satellite evidence that *E.*
772 *huxleyi* phytoplankton blooms weaken marine carbon sinks, Geophys. Res. Lett.,
773 45, e2017GL076240, doi: 10.1002/2017GL076240, 2018.
774 Kottmeier, D. M., Rokitta, S. D., and Rost, B.: Acidification, not carbonation, is the
775 major regulator of carbon fluxes in the coccolithophore *Emiliania huxleyi*, New

Phytol., 211, 126–137, doi: 10.1111/nph.13885, 2016.

Kubryakova, E. A., Kubryakov, A. A., and Mikaelyan, A. S.: Winter coccolithophore blooms in the Black Sea: Interannual variability and driving factors, J. Mar. Syst., 213, 103461, doi: 10.1016/j.jmarsys.2020.103461, 2021.

~~Larsen, A., Flaten, G. A. F., Sandaa, R., Castberg, T., Thyrhaug, R., Erga, S. R., Jacquet, S., and Bratbak, G.: Spring phytoplankton bloom dynamics in Norwegian coastal waters: Microbial community succession and diversity, Limnol. Oceanogr., 49, 180–190, doi: 10.4319/lo.2004.49.1.0180, 2004.~~

Leonardos, K., and Geider, R. J.: Elevated atmospheric carbon dioxide increases organic carbon fixation by *Emiliania huxleyi* (haptophyta), under nutrient-limited high-light conditions, J. Phycol., 41, 1196–1203, doi: 10.1111/j.1529-8817.2005.00152.x, 2005.

Lohbeck, K., Riebesell, U., and Reusch, T. B. H.: Gene expression changes in the coccolithophore *Emiliania huxleyi* after 500 generation of selection to ocean acidification, Proc. R. Soc. B., 281, 20140003, doi: 10.1098/rspb.2014.0003, 2014.

Lu, Y., Wen, Z., Shi, D., Chen, M., Zhang, Y., Bonnet, S., Li, Y., Tian, J., and Kao, S. J.: Effect of light on N_2 fixation and net nitrogen release of *Trichodesmium* in a field study, Biogeosciences, 15, 1–12, doi: 10.5194/bg-15-1-2018, 2018.

Mackinder, L., Wheeler, G., Schroeder, D., von Dassow, P., Riebesell, U., and Brownlee, C.: Expression of biomineralization-related ion transport genes in *Emiliania huxleyi*, Env. Microbiol., 13, 3250–3565, doi:10.1111/j.1462-2920.2011.02561.x, 2011.

Masuko, T., Minami, A., Iwasaki, N., Majima, T., Nishimura, S. I., and Lee, Y. C.: Carbohydrate analysis by a phenol-sulfuric acid method in microplate format,

Anal. Biochem., 339, 69–72, doi: 10.1016/j.ab.2004.12.001, 2005.

Matthiessen, B., Eggers, S. L., and Krug, S. A.: High nitrate to phosphorus regime attenuates negative effects of rising pCO_2 on total population carbon accumulation, Biogeosciences, 9, 1195–1203, doi: 10.5194/bg-9-1195-2012, 2012.

McKew, B. A., Metodieva, G., Raines, C. A., Metodiev, M. V., and Geider, R. J.: Acclimation of *Emiliania huxleyi* (1516) to nutrient limitation involves precise modification of the proteome to scavenge alternative sources of N and P, Environ. Microbiol., 17, 4050–4062, doi: 10.1111/1462-2920.12957, 2015.

Meyer, J., and Riebesell, U.: Reviews and syntheses: responses of coccolithophores to ocean acidification: a meta-analysis, Biogeosciences, 12, 1671–1682, doi: 10.5194/bg-12-1671-2015, 2015.

Moreno, A. R., and Martiny, A. C.: Ecological stoichiometry of ocean plankton, Ann. Rev. Mar. Sci., 10, 43–69, doi: 10.1146/annurev-marine-121916-063126, 2018.

Müller, M. N., Antia, A. N., and LaRoche, J.: Influence of cell cycle phase on calcification in the coccolithophore *Emiliania huxleyi*, Limnol. Oceanogr., 53, 506–512, doi: 10.4319/lo.2008.53.2.0506, 2008.

Ni, G., Zimbalatti, G., Murphy, C. D., Barnett, A. B., Arsenault, C. M., Li, G., Cockshutt, A. M., and Campbell, D. A.: Arctic *Micromonas* uses protein pools and non-photochemical quenching to cope with temperature restrictions on Photosystem II protein turnover, Photosynth. Res., 131, 203–220, doi: 10.1007/s11120-016-0310-6, 2016.

Pakulski, J. D., and Benner, R.: An improved method for the hydrolysis and MBTH analysis of dissolved and particulate carbohydrates in seawater, Mar. Chem., 40, 143–160, doi: 10.1016/0304-4203(92)90020-B, 1992.

826 Perrin, L., Probert, I., Langer, G., and Aloisi, G.: Growth of the coccolithophore
827 *Emiliania huxleyi* in light- and nutrient-limited batch reactors: relevance for the
828 BIOSOPE deep ecological niche of coccolithophores, Biogeosciences, 13, 5983–
829 6001, doi: 10.5194/bg-13-5983-2016, 2016.
830 Pierrot, D., Lewis, E., and Wallace, D. W. R.: MS Excel program developed for CO_2
831 system calculations, ORNL/CDIAC-105, Carbon Dioxide Information Analysis
832 Centre, Oak Ridge National Laboratory, U.S., Department of Energy, doi:
833 10.3334/CDIAC/otg.CO2SYS_XLS_CDIAC105a, 2006.
834 R version 3.5.0.: The R foundation for statistical computing platform,
835 x86_64-w64-mingw32/x64. Available from:
836 https://cran.r-project.org/bin/windows/ base/old/3.5.0, 2018.
837 Reith, M. E., and Cattolico, R. A.: Chloroplast protein synthesis in the chromophytic
838 alga *Olisthodiscus luteus*, Plant Physiol., 79, 231–236, doi: 10.1104/pp.79.1.231,
839 1985.
840 Riebesell, U., Bach, L. T., Bellerby, R. G. J., Rafael Bermúdez Monsalve, J.,
841 Boxhammer, T., Czerny, J., Larsen, A., Ludwig, A., and Schulz, K. G.:
842 Competitive fitness of a predominant pelagic calcifier impaired by ocean
843 acidification, Nat. Geosci., 10, 19–24, dio: 10.1038/NGEO2854, 2017.
844 Riegman, R., Stolte, W., Noordeloos, A. A. M., and Slezak, D.: Nutrient uptake and
845 alkaline phosphatase (EC 3:1:3:1) activity of *Emiliania huxleyi*
846 (Prymnesiophyceae) during growth under N and P limitation in continuous
847 cultures, J. Phycol., 36, 87–96, 2000.
848 Rokitta, S. D., von Dassow, P., Rost, B., and John, U.: P- and N-depletion trigger
849 similar cellular responses to promote senescence in eukaryotic phytoplankton,
850 Front. Mar. Sci., 3, 109, doi: 10.3389/fmars.2016.00109, 2016

Rokitta, S. D., and Rost, B: Effects of CO_2 and their modulation by light in the life-cycle stages of the coccolithophore *Emiliania huxleyi*, Limnol. Oceanog., 57, 607–618, doi: 10.4319/lo.2012.57.2.0607, 2012.

Rokitta, S. D., de Nooijer, L. J., Trimborn, S., de Vargas, C., Rost, B., and John, U.: Transcriptome analyses reveal differential gene expression patterns between the life-cycle stages of *Emiliania huxleyi* (haptophyta) and reflect specialization to different ecological niches, J. Phycol., 47, 829–838, doi: 10.1016/S0924-9338(02)00624-7, 2011.

Rost, B., and Riebesell, U.: Coccolithophores and the biological pump: responses to environmental changes, in: Coccolithophores : from molecular biology to global impact, edited by: Thierstein, H. R. and Young, J. R., Springer, Berlin, 99–125, 2004.

Rouco, M., Branson, O., Lebrato, M., and Iglesias-Rodr ́guez, M.: The effect of nitrate and phosphate availability on *Emiliania huxleyi* (NZEH) physiology under different CO_2 scenarios, Front. Microbiol., 4, 1–11, doi: 10.3389/fmicb.2013.00155, 2013.

Roy, R. N., Roy, L. N., Vogel, K. M., Porter-Moore, C., Pearson, T., Good, C. E., Millero, F. J., and Campbell, D. C.: Thermodynamics of the dissociation of boric acid in seawater at S 5 35 from 0 degrees C to 55 degrees C, Mar. Chem., 44, 243–248, doi: 10.1016/0304-4203(93)90206-4, 1993.

Shemi, A., Schatz, D., Fredricks, H. F., Van Mooy, B. A. S., Porat, Z., and Vardi, A.: Phosphorus starvation induces membrane remodeling and recycling in *Emiliania huxleyi*, New Phytol., 211, 886–898, doi: 10.1111/nph.13940, 2016.

874 Solórzano, L., and Sharp, J. H.: Determination of total dissolved phosphorus and
875 particulate phosphorus in nature waters, Limnol. Oceanogr., 25, 754–758, doi:
876 10.4319/lo.1980.25.4.0754, 1980.
877 Steinacher, M., Joos, F., Frölicher, T. L., Bopp, L., Cadule, P., Cocco, V., Doney, S.
878 C., Gehlen, M., Lindsay, K., Moore, J. K., Schneider, B., and Segschneider, J.:
879 Projected 21st century decrease in marine productivity: a multi-model analysis,
880 Biogeosciences, 7, 979–1005, doi: 10.5194/bg-7-979-2010, 2010.
881 Sterner, R. W., and Elser, J. J.: Ecological Stoichiometry: The Biology of Elements
882 from Molecules to the Biosphere, Princeton University Press, Princeton, 2002.
883 Terrats, L., Claustre, H., Cornec, M., Mangin, A., and Neukermans, G.: Detection of
884 coccolithophore blooms with BioGeoChemical-Argo floats, Geophys. Res. Lett.,
885 47, e2020GL090559, doi: 10.1029/2020GL090559, 2020.
886 Townsend, D. W., Keller, M. D., Holligan, P. M., Ackleson, S. G., and Balch, W. M.:
887 Blooms of the coccolithophore *Emiliania huxleyi* with respect to hydrography in
888 the Gulf of Maine, Cont. Shelf Res., 14, 979–1000, doi:
889 10.1016/0278-4343(94)90060-4, 1994.
890 Tyrrell, T., and Merico, A.: *Emiliania huxleyi*: bloom observations and the conditions
891 that induce them, in: Coccolithophores : from molecular biology to global impact,
892 edited by: Thierstein, H. R. and Young, J. R., Springer, Berlin, 75–97, 2004.
893 Wang, C., Wang, J., Li, L., Wang, Y., and Lin, S.: P-limitation promotes carbon
894 accumulation and sinking of *Emiliania huxleyi* through transcriptomic
895 reprogramming, Front. Mar. Sci., 9, 860222, doi: 10.3389/fmars.2022.860222,
896 2022.
897 Wang, G., Xie, S. P., Huang, R. X., and Chen. C.: Robust warming pattern of global
898 subtropical oceans and its mechanism, J. Climate, 28, 8574–8584, doi:

10.1175/jcli-d-14-00809.1, 2015.

Wilson, D. N., and Doudna Cate J. H.: The structure and function of the eukaryotic ribosome, CSH Perspect. Biol., 4, a011536, doi: 10.1101/cshperspect.a011536, 2012.

Zhang, Y., Collins, S., and Gao, K.: Reduced growth with increased quotas of particulate organic and inorganic carbon in the coccolithophore *Emiliania huxleyi* under future ocean climate change conditions, Biogeosciences, 17, 6357–6375, doi: 10.5194/bg-17-6357-2020, 2020.

Zhang, Y., Li, Z. K., Schulz, K. G., Hu, Y., Irwin, A. J., and Finkel, Z. V.: Growth-dependent changes in elemental stoichiometry and macromolecular allocation in the coccolithophore *Emiliania huxleyi* under different environmental conditions, Limnol. Oceanogr., 66, 2999–3009, doi: 10.1002/lno.11854, 2021.

Figure Legends

Figure 1. Growth rate (**a**), cellular contents of particulate organic carbon (POC, **b**), nitrogen (PON, **c**) and phosphorus (POP, **d**), and particulate inorganic carbon (PIC, **e**) of *Emiliania huxleyi* RCC1266 in the treatments of high phosphorus availability and low CO_2 level (HP+LC), high phosphorus availability and high CO_2 level (HP+HC), low phosphorus availability and low CO_2 level (LP+LC), and low phosphorus availability and high CO_2 level (LP+HC) under low light (empty, 40 μmol photons m^{-2} s^{-1}) and high light (fill, 300 μmol photons m^{-2} s^{-1}) intensities. Different letters represent significant differences in each parameters between treatments ($p < 0.05$). The data represents the means and standard deviation of four independent cultures.

Figure 2. Cellular contents of carbohydrate (**a**) and protein (**b**), and the percentages of POC allocated to carbohydrate (**c**) and protein (**d**), and the percentage of PON allocated to protein (**e**) of *E. huxleyi* RCC1266 in the treatments of high phosphorus availability and low CO_2 level (HP+LC), high phosphorus availability and high CO_2 level (HP+HC), low phosphorus availability and low CO_2 level (LP+LC), and low phosphorus availability and high CO_2 level (LP+HC) under low light (empty) and high light (fill) intensities. Different letters represent significant differences in each parameters between treatments ($p < 0.05$). The data represents the means and standard deviation of four independent cultures. ~~Please see figure 1 for more detailed information.~~

Figure 3. Cellular POC : POP ratio (**a**), PON : POP ratio (**b**), and protein content (**c**) of *E. huxleyi* RCC1266 as a function of growth rate, and cellular POC content as a function of carbohydrate (**d**) in the treatments of high phosphorus availability and low

CO_2 level (HP+LC, □), high phosphorus availability and high CO_2 level (HP+HC, ○), low phosphorus availability and low CO_2 level (LP+LC, △), and low phosphorus availability and high CO_2 level (LP+HC, ◇) under low light (LL, empty) and high light (HL, fill) intensities. Each point indicates an individual replicate under each treatment. ~~Please see figure 1 for more detailed information.~~

Table 1. Carbonate chemistry parameters and dissolved inorganic phosphorus (DIP) concentration at the end of the incubation. The values are means ± standard deviation (sd) of four replicates. Respectively, LL and HL represent 40 and 300 µmol photons m^{-2} s^{-1} of photosynthetically active radiation (PAR), and HP and LP represent 4 and 0.43 µmol L^{-1} PO_4^{3-} at the beginning of the incubations.

			pCO_2 (µatm)	pH (total scale)	TA (µmol L^{-1})	DIC (µmol L^{-1})	HCO_3^- (µmol L^{-1})	CO_3^{2-} (µmol L^{-1})	DIP (µmol L^{-1})
LL	HP	LC	403±4	8.06±0.01	2346±23	2074±21	1861±18	200±2	3.20±0.03
		HC	881±20	7.77±0.01	2351±33	2216±32	2074±30	114±2	3.12±0.08
	LP	LC	329±4	8.13±0.01	2332±24	2024±22	1787±19	225±3	<0.04
		HC	730±8	7.84±0.01	2349±24	2189±23	2033±22	132±2	<0.04
HL	HP	LC	357±9	8.09±0.01	2235±41	1959±35	1749±30	199±6	2.86±0.06
		HC	791±7	7.80±0.01	2296±20	2151±20	2007±18	118±1	2.70±0.06
	LP	LC	303±4	8.16±0.01	2354±13	2024±11	1773±9	241±3	<0.04
		HC	735±19	7.83±0.01	2319±69	2162±65	2011±60	128±5	<0.04

Table 2. Growth rate (d^{-1}), cellular contents of POC, PON, POP, PIC, carbohydrate (CHO) and protein (Pro) (pg $cell^{-1}$), and the ratios of POC : PON, POC : POP, PON : POP and PIC : POC, and the percentages of POC allocated to carbohydrate (CHO–C : POC) and protein (Pro–C : POC), and the percentage of PON allocated to protein (Pro–N : PON) (%). LC and HC represent low CO_2 (426 μatm) and high CO_2 (946 μatm) levels, respectively. Please see table 1 for more detailed information.

	Low light intensity				High light intensity			
	HP		LP		HP		LP	
	LC	HC	LC	HC	LC	HC	LC	HC
Growth rate	0.91±0.03	0.88±0.01	0.83±0.02	0.70±0.03	1.35±0.03	1.33±0.02	1.34±0.02	1.12±0.02
POC	8.34±0.57	8.73±0.32	8.20±0.36	8.04±0.24	10.53±0.70	11.04±0.42	11.73±0.19	12.70±0.50
PON	1.49±0.16	1.58±0.12	1.23±0.06	1.20±0.10	1.65±0.05	1.89±0.07	1.51±0.07	1.56±0.06
POP	0.16±0.01	0.15±0.01	0.08±0.01	0.07±0.01	0.22±0.01	0.21±0.01	0.12±0.01	0.10±0.01
PIC	2.12±0.22	1.45±0.17	2.44±0.11	2.06±0.37	3.74±0.22	2.41±0.41	4.83±0.34	3.79±0.49
POC:PON	6.57±0.43	6.46±0.52	7.78±0.46	7.87±0.54	7.45±0.28	6.83±0.32	9.09±0.44	9.50±0.11
POC:POP	133.3±7.8	153.8±13.9	282.4±31.2	313.0±40.5	124.2±3.5	137.8±8.5	259.7±23.2	316.9±30.4
PON:POP	20.40±2.53	23.98±3.37	36.30±3.54	40.10±7.42	16.68±0.47	20.21±1.47	28.63±2.80	33.33±2.85
PIC:POC	0.26±0.04	0.17±0.02	0.30±0.02	0.26±0.04	0.36±0.02	0.22±0.04	0.41±0.03	0.30±0.04
CHO	1.45±0.15	1.81±0.16	1.79±0.16	1.94±0.16	3.58±0.41	4.30±0.17	4.96±0.24	5.85±0.49
Protein	5.23±0.55	5.37±0.39	3.73±0.27	3.80±0.15	6.45±0.36	6.97±0.22	6.25±0.29	6.28±0.30
CHO–C:POC	6.95±0.41	8.31±0.85	8.71±0.70	9.64±0.58	13.62±1.43	15.60±0.98	16.92±1.04	18.39±0.96
Pro–C:POC	33.26±3.24	32.58±1.98	24.15±2.52	25.07±1.69	32.49±1.69	33.51±1.41	28.23±1.35	26.21±1.27
Pro–N:PON	56.84±8.96	54.55±6.51	48.41±2.46	51.07±5.40	62.62±2.88	59.12±1.21	66.35±4.06	64.44±2.73

1009

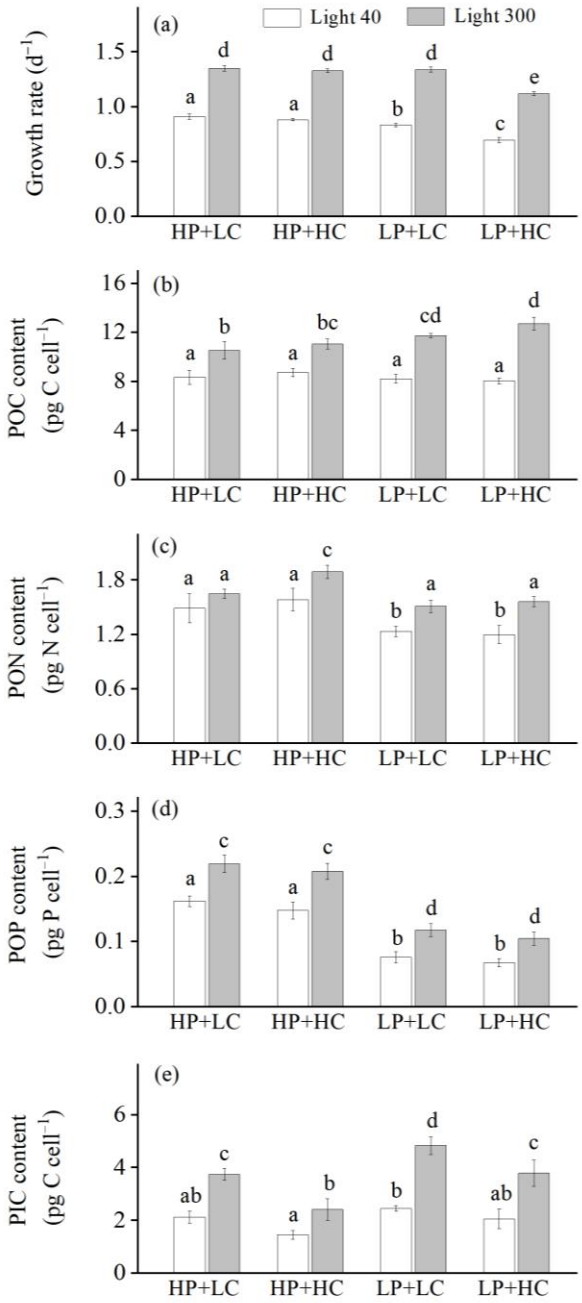

1010

1011

1012 Figure 1

1013

1014

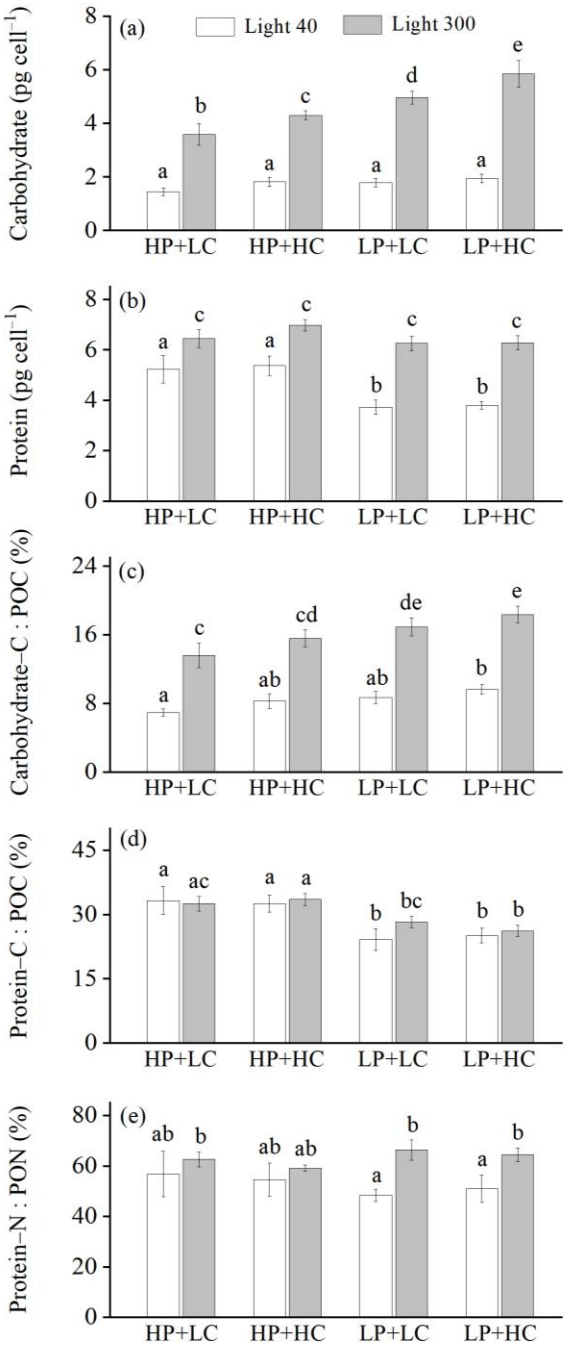
(a)
Light 40
Light 300
Carbohydrate (pg cell^{-1})
(b)
Protein (pg cell^{-1})
(c)
Carbohydrate–C : POC (%)
(d)
Protein–C : POC (%)
(e)
Protein–N : PON (%)
HP+LC
HP+HC
LP+LC
LP+HC

Figure 2

1021

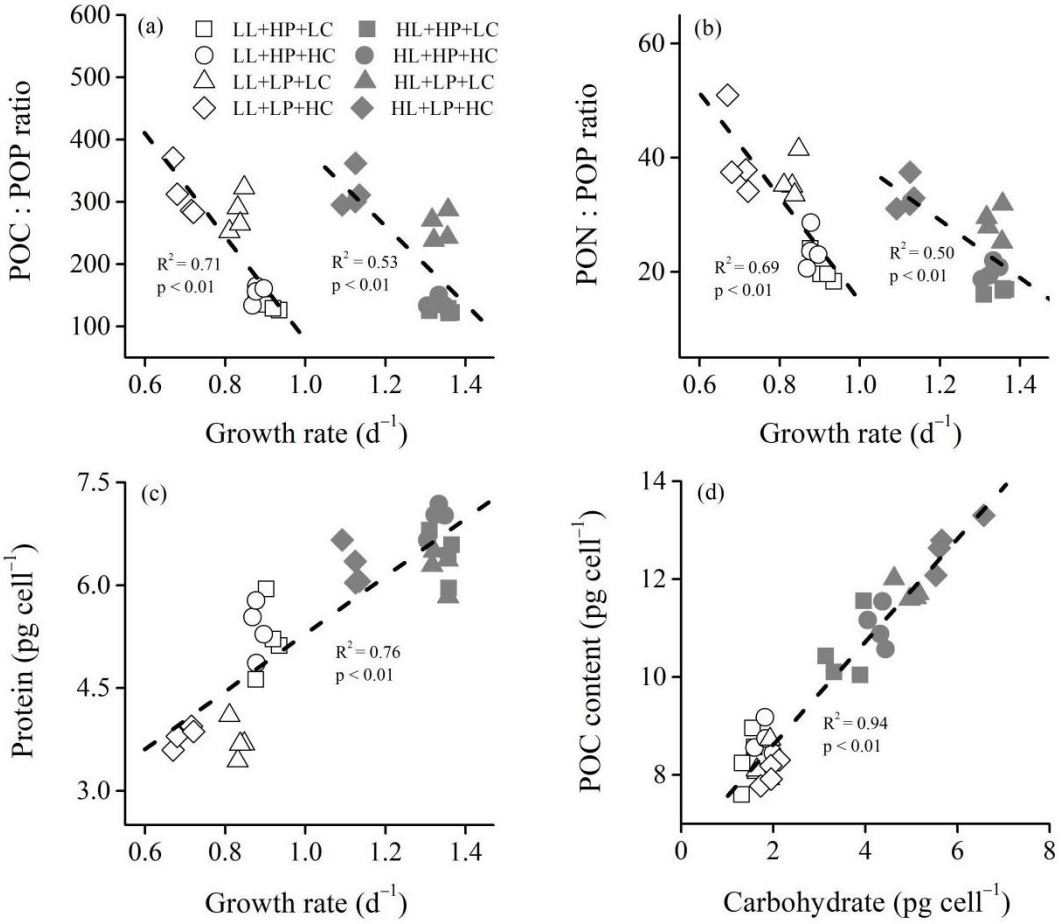

1022

1023

1024 Figure 3

1025

1026

Supplemental Information

Materials and Methods

1 RNA Analyses

Total RNA was extracted by using TRIzol reagent (Invitrogen) and the RNeasy Plus Mini Kit (Qiagen). Samples were resuspended in 1.2 mL TRIzol reagent (Thermo Fisher Scientific) in lysing matrix D tubes (MP Biomedicals), homogenized by a FastPrep-24 machine (MP Biomedicals, 3 cycles, 8.0 m s^{-1}, 30 s, 3 min ice-chilling at interval), followed by centrifugation at 12,000 × g for 3 min at 4 ºC (Eppendorf 5430R). RNA was extracted using a standard phenol-chloroform method (Chomczynski and Sacchi 1987). For more detail information, please see Zhang et al. (2021).

2 Bioinformatics

The quality of the raw reads was assessed by Fastqc v.0.11.8 (Andrews, 2010) and Fastq screen v.0.13.0 (Wingett and Andrews, 2018) and summarized using Multiqc (Ewels et al., 2016). Trimming of the raw reads was performed to remove low-quality bases and adapter sequences with Trimmomatic v.0.38 (Bolger et al., 2014). *De novo* transcriptome assembly was performed with the Trinity's version 2.11.0 (Grabherr et al., 2011), and the low-quality assembly were removed with CD-HIT (Li and Godzik, 2006). A preliminary assessment of *de novo* assembly quality was performed with Transrate (Smith-Unna et al., 2016) and Busco (Hara et al., 2015), and the completeness assessment yielded high scores for all assemblies. Open reading frames (ORFs) were then predicted using TransDecoder version v5.5.0 (Haas et al., 2013), and were then annotated by Blastx, Hmmpress, Signalp, Rnammer, PFam (Lagesen et al., 2007). All annotations were loaded and integrated with Trinotate v3.0.0 (Haas et

al., 2013). ORFs were further functionally annotated and assigned to the KEGG and GhostKOALA (Moreno-Santillán et al., 2019). Cleaned and trimmed reads of each sample were mapped to the assembled transcriptomes by salmon v0.9.1 (Patro et al., 2017). The differential expression was them calculated by DESeq2 v1.24.0 (Love et al., 2014) with a Benjamini-Hochberg adjusted p-value < 0.05. Data analysis and visualizations were made using R v.3.6.1 (Team, 2020), packages ggplot2 v.3.2.0 (Wickham, 2016) and Pheatmap v.1.0.12 (Kolde, 2015).

Table S1. Results of three-way ANOVAs of the effects of light intensity (L), dissolved inorganic phosphorus (PO_4^{3-}) concentration (P), pCO_2 level (C), and their interaction on growth rate, cellular contents of POC, PON, POP, PIC, carbohydrate and protein, and the ratios of POC : PON, POC : POP, PON : POP and PIC : POC, and the percentages of POC allocated to carbohydrate (carbohydrate–C : POC) and protein (protein–C : POC), and the percentage of PON allocated to protein (protein–N : PON). Please see figure 1 for more detailed information.

Parameter		L	P	C	L×P	L×C	P×C	L×P×C
Growth rate	F	4588.5	198.3	225.7	6.7	14.7	100.9	8.6
	p	<0.01	<0.01	<0.01	=0.02	<0.01	<0.01	<0.01
POC	F	864.7	0.6	0.6	36.4	8.1	0.2	2.6
	p	<0.01	=0.46	=0.46	<0.01	<0.01	=0.65	=0.12
PON	F	172.2	70.6	17.7	1.2	6.3	10.0	0.2
	p	<0.01	<0.01	<0.01	=0.33	=0.02	<0.01	=0.65
POP	F	188.3	724.8	8.2	6.6	0.1	0.2	0.2
	p	<0.01	<0.01	<0.01	=0.02	=0.89	=0.65	=0.65
PIC	F	329.4	109.1	47.2	17.7	8.9	1.9	0.1
	p	<0.01	<0.01	<0.01	<0.01	<0.01	=0.17	=0.98
POC : PON	F	207.6	396.4	0.1	14.9	0.2	9.3	2.1
	p	<0.01	<0.01	=0.96	<0.01	=0.65	<0.01	=0.16
POC : POP	F	7.7	351.3	18.7	0.1	0.3	2.6	1.0
	p	=0.01	<0.01	<0.01	=0.85	=0.62	=0.12	=0.32
PON : POP	F	29.4	183.1	29.9	1.9	0.1	0.3	0.1
	p	<0.01	<0.01	<0.01	=0.18	=0.97	=0.61	=0.94
PIC : POC	F	90.2	71.9	77.6	0.6	6.6	2.4	0.3
	p	<0.01	<0.01	<0.01	=0.46	=0.02	=0.14	=0.61
Carbohydrate	F	925.2	37.7	23.6	40.9	7.9	0.9	0.9
	p	<0.01	<0.01	<0.01	<0.01	<0.01	=0.34	=0.34
Protein	F	782.4	77.0	1.0	21.1	0.8	2.0	0.8
	p	<0.01	<0.01	=0.34	<0.01	=0.38	=0.17	=0.37
Carbohydrate–C : POC	F	793.3	76.2	17.1	4.9	0.7	0.6	0.1
	p	<0.01	<0.01	<0.01	=0.04	=0.41	=0.43	=0.95
Protein–C : POC	F	6.3	120.0	0.7	2.4	0.6	2.2	2.7
	p	=0.02	<0.01	=0.42	=0.13	=0.45	=0.15	=0.11
Protein–N : PON	F	36.3	4.3	2.8	9.2	0.7	0.7	0.2
	p	<0.01	=0.05	=0.10	<0.01	=0.41	=0.41	=0.63

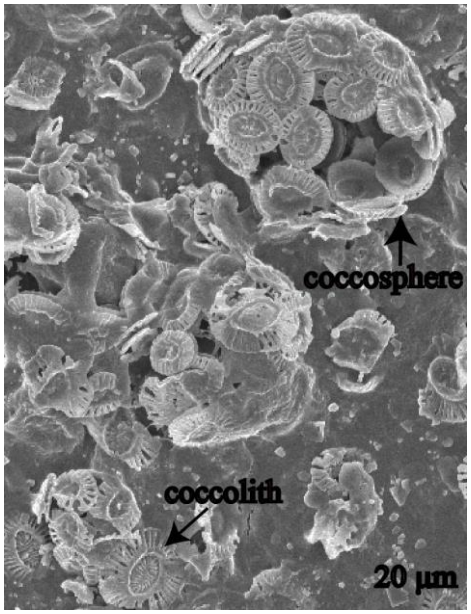

Figure S1. A scanning electron microscopy (SEM) picture of the coccosphere and coccolith of *E. huxleyi* RCC 1266.

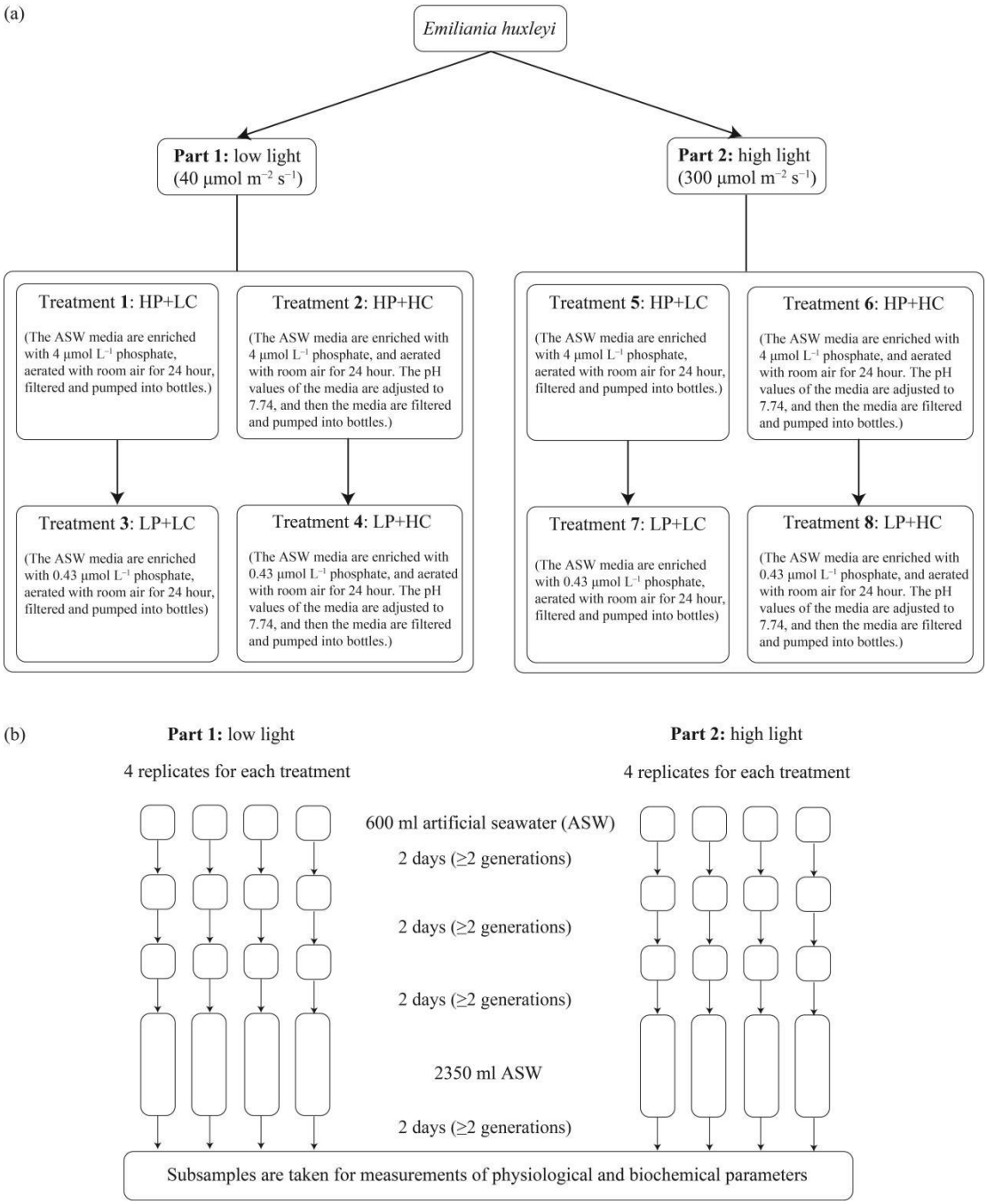

Figure S2~~1~~. Flow chart of the experimental processes (**a**) and flow chart of the pre-culture and experimental cultures in each treatment (**b**). At the beginning of the incubations, HP and LP represent 4 and 0.43 µmol L^{-1} PO_4^{3-}, and LC and HC represent low (about 426 µatm) and high CO_2 (about 946 µatm) concentrations, respectively.

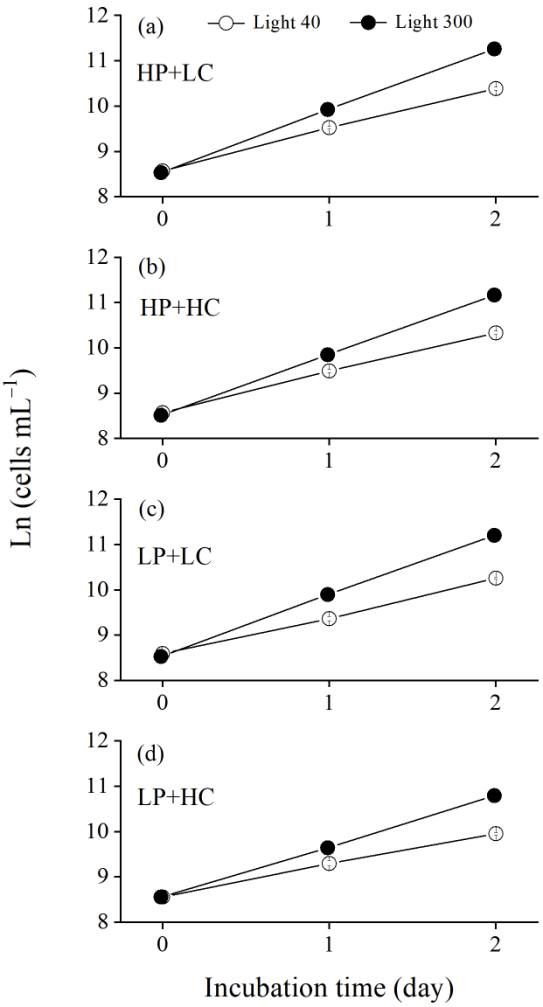

Figure S3~~2~~. Cell density of *E. huxleyi* RCC1266 in the treatments of HP+LC, HP+HC, LP+LC and LP+HC under low light (empty) and high light (fill) intensities during the experimental cultures. The cells were inoculated to achieve an initial density of about 5000 cell mL^{-1}, and cultured in each experimental condition for 2 days and then diluted to the initial cell density again. This process was repeated four times. The data represents the means and standard deviation of four independent cultures in the fourth incubation. Please see figure 1 for more detailed information.

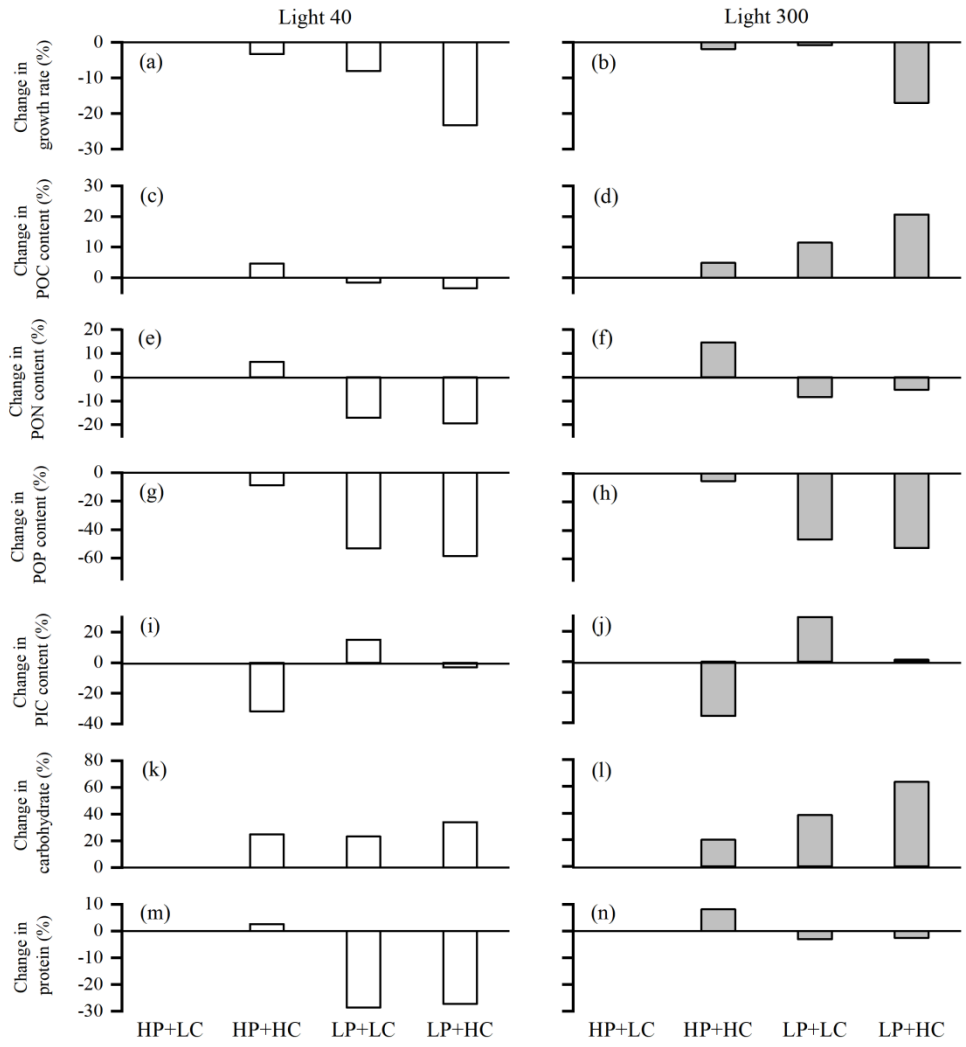

Figure S43. In comparison to the HP+LC treatment, changes in growth rate (**a**, **b**) and cellular contents of POC (**c**, **d**), PON (**e**, **f**), POP (**g**, **h**), PIC (**i**, **j**), carbohydrate (**k**, **l**) and protein (**m**, **n**) of *E. huxleyi* RCC1266 in the treatments of HP+HC, LP+LC and LP+HC under low light (empty) and high light (fill) intensities. The data represents the means of four independent cultures. Please see figure 1 for more detailed information.

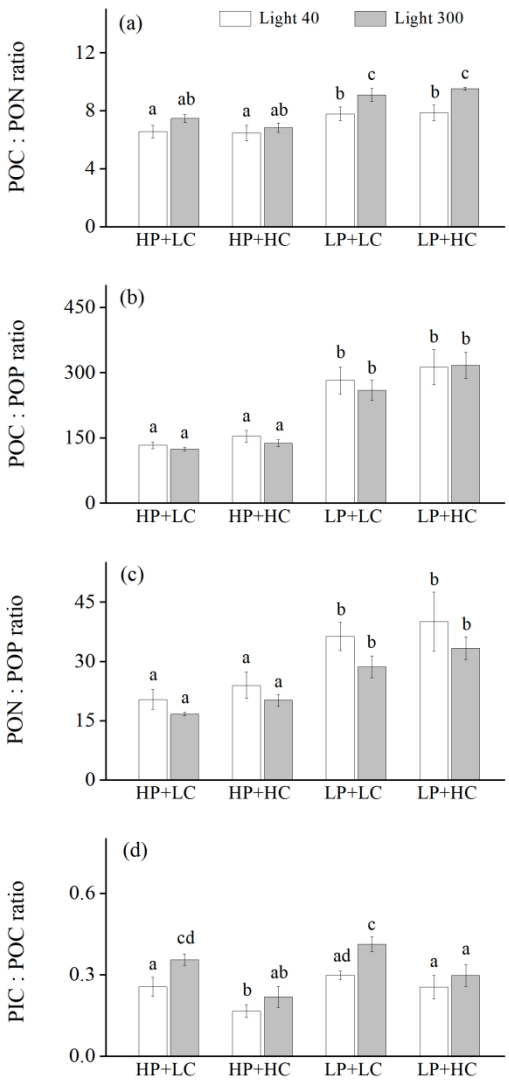

Figure S54. The ratios of POC : PON (**a**), POC : POP (**b**), PON : POP (**c**) and PIC : POC (**d**) of *E. huxleyi* RCC1266 in the treatments of HP+LC, HP+HC, LP+LC and LP+HC under low light (empty) and high light (fill) intensities. Different letters represent significant differences in each parameters between treatments ($p < 0.05$). The data represents the means and standard deviation of four independent cultures. Please see figure 1 for more detailed information.

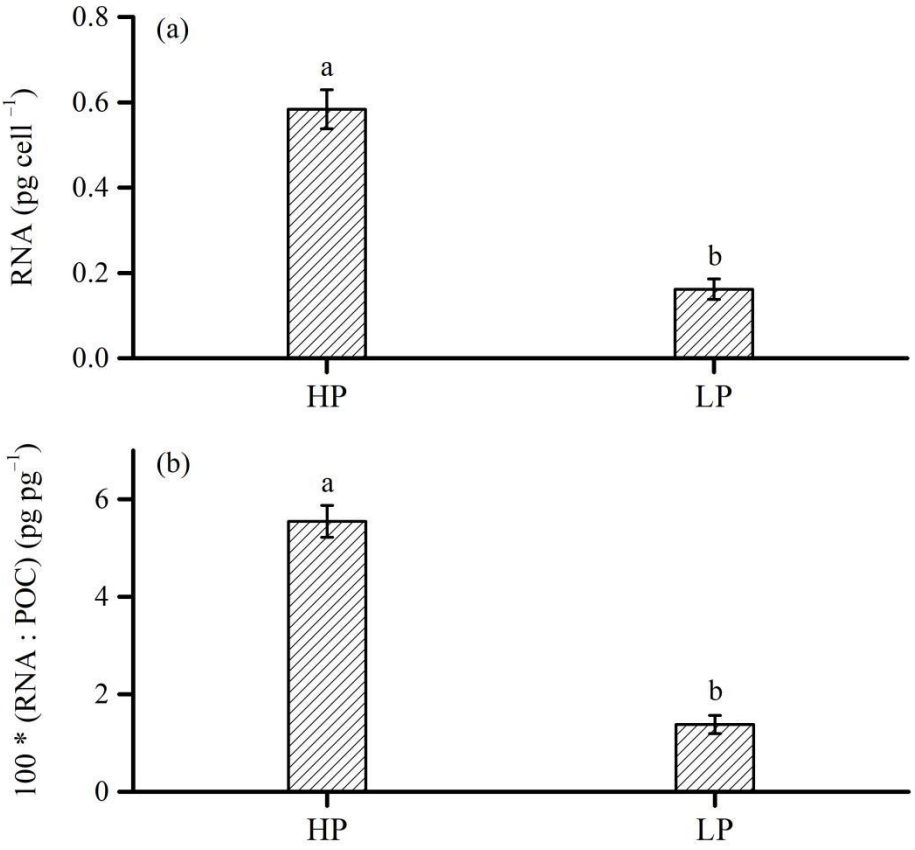

Figure S65. Cellular RNA content (**a**) and POC normalized RNA content (**b**) of *E. huxleyi* RCC1266 in the treatments of HP+LC and LP+LC under high light intensity. Different letters in each panel represent significant differences between treatments ($p < 0.05$). The data represents the means and standard deviation of four independent cultures. Please see figure 1 for more detailed information.

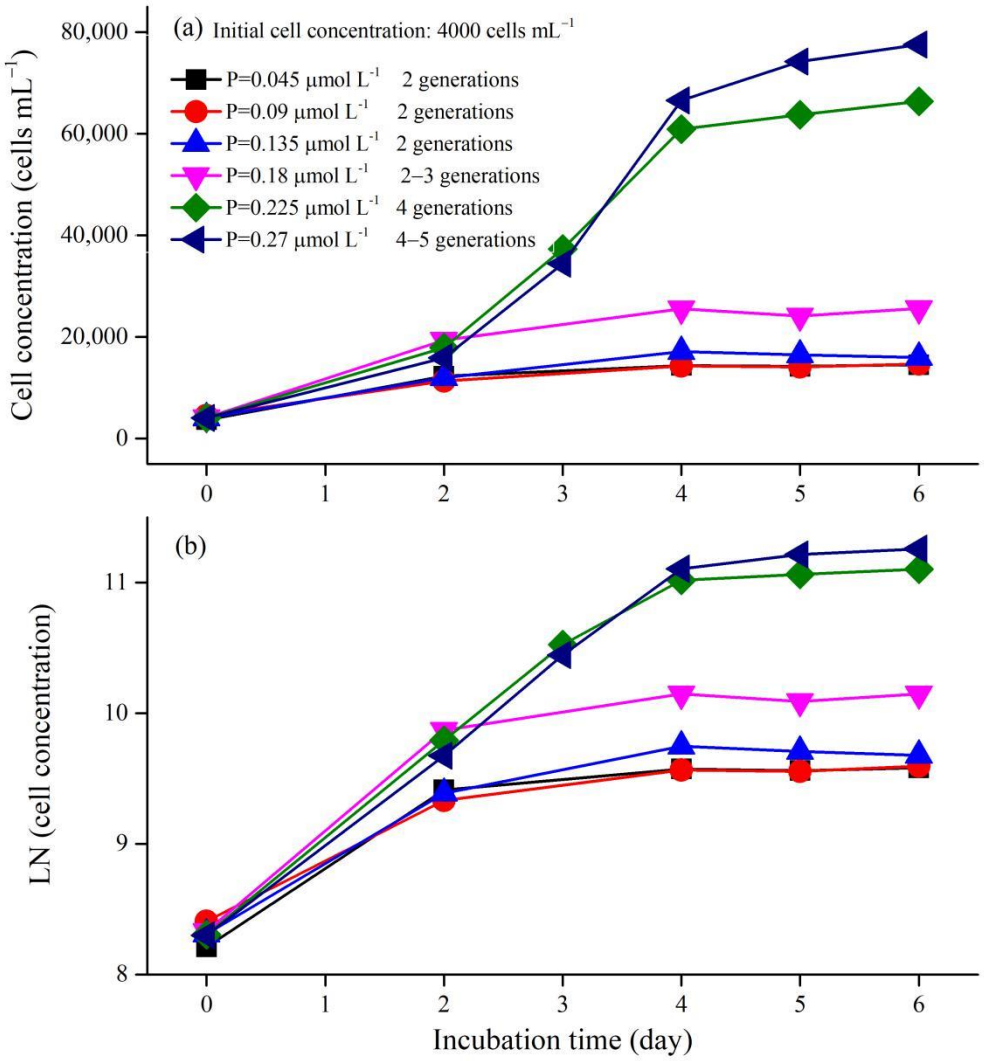

Figure S6. Cell density of *E. huxleyi* RCC1266 under different phosphorus concentrations (P) at 150 μmol photons m^{-2} s^{-1} of photosynthetically active radiation under low CO_2 level.

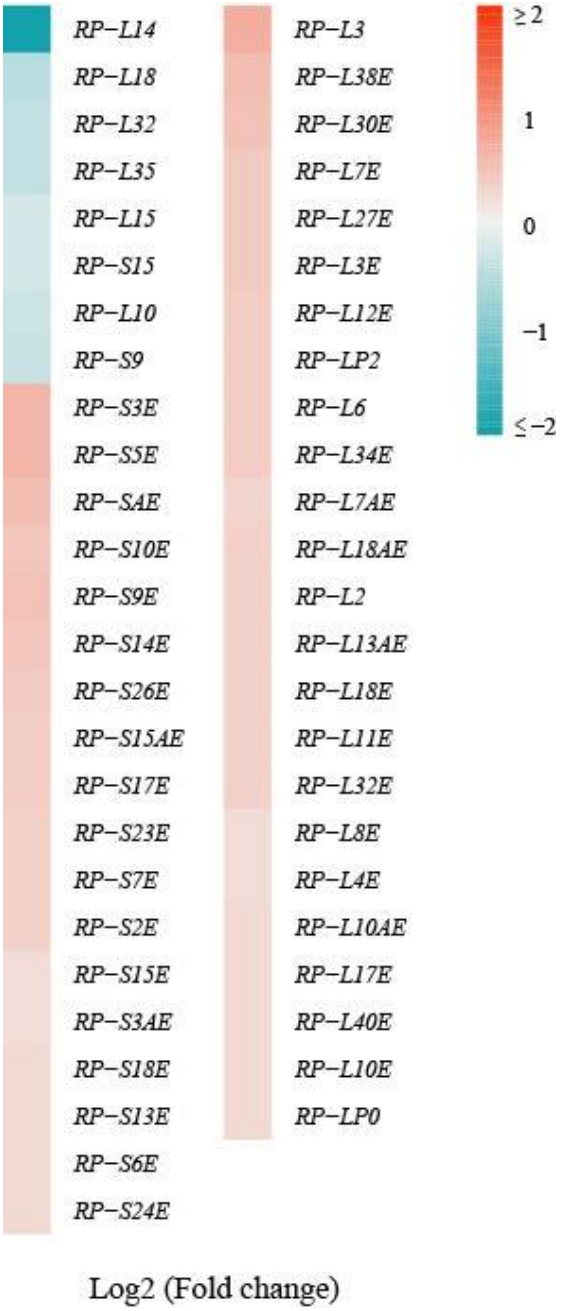

Figure S7. Heatmap of significant change in expression of genes linked to ribosome metabolism (Ribosome_ko03010) under the low pH treatment (ocean acidification) in comparison to the high pH treatment (present CO_2 level). Red indicates up-regulation of gene, and blue indicates down-regulation of gene. *RP-S* presents genes linked to small subunit ribosomal protein, and *RP-L* presents genes linked to large subunit ribosomal protein.

References

Andrews, S.: FASTQC: a quality control tool for high throughput sequence data, Cambridge, 2010. https://www.bioinformatics.babraham.ac.uk/projects/fastqc/.

Bolger, A. M., Lohse, M., and Usadel, B.: TRIMMOMATIC : a flexible trimmer for illumina sequence data, Bioinformatics, 30, 2114–2120, 2014.

Chomczynski, P., and Sacchi, N.: Single-step method of RNA isolation by acid guanidinium thiocyanate-phenol-chloroform extraction, Anal. Biochem., 162, 156–159, doi: 10.1006/abio.1987.9999, 1987.

Ewels, P., Magnusson, M., Lundin, S., and Käller, M.: MULTIQC: summarize analysis results for multiple tools and samples in a single report, Bioinformatics, 32, 3047–3048, 2016.

Grabherr, M. G., Haas, B. J., Yassour, M., Levin, J. Z., Thompson, D. A., Amit, I., Adiconis, X., Fan, L., Raychowdhury, R., Zeng, Q., Chen, Z., Mauceli, e., Hacohen, N., Gnirke, A., Rhind, N., di Palma, F., Birren, B. W., Nusbaum, C., Lindblad-Toh, K., Friedman, N, and Regev, A.: Full-length transcriptome assembly from RNA-Seq data without a reference genome, Nat. Biotechnol., 29, 644–652, 2011.

Haas, B. J., Papanicolaou, A., Yassour, M., Grabherr, M., Blood, P. D., Bowden, J., Couger, M. B., Eccles, D., Li, B., Lieber M., MacManes, M. D., Ott, M., Orvis, J., Pochet, N., Strozzi, F., Weeks, N., Westerman, R., Willian, T., Dewey, C. N., Henschet, R., LeDuc, R. D., Friedman, N., and Regev, A: *De novo* transcript sequence reconstruction from RNA-seq using the Trinity platform for reference generation and analysis, Nat. Protoc., 8, 1494–1512, 2013.

Hara, Y., Tatsumi, K., Yoshida, M., Kajikawa, E., Kiyonari, H., and Kuraku, S.: Optimizing and benchmarking *de novo* transcriptome sequencing: from library

preparation to assembly evaluation, BMC Genomics, 16, 977, 2015.

Kolde, R.: Package 'pheatmap'. R. Package, 1, 790, 2015.

Lagesen, K., Hallin, P., Rodland, E. A., Staerfeldt, H. H., Rognes, T., and Ussery, D. W.: RNAmmer: Consistent and rapid annotation of ribosomal RNA genes, Nucleic Acids Res., 35, 3100–3108, 2007.

Li, W., and Godzik, A.: Cd-hit: A fast program for clustering and comparing large sets of protein or nucleotide sequences, Bioinformatics, 22, 1658–1659, 2006.

Love, M. I., Huber, W., and Anders, S.: Moderated estimation of fold change and dispersion for RNA-seq data with DES EQ 2, Genome Biol., 15, 550, 2014.

Moreno-Santillán, D. D., Machain-Williams, C., Hernández-Montes, G., and Ortega, J.: *De novo* transcriptome assembly and functional annotation in five species of bats, Sci. Rep., 9, 6222, 2019.

Patro, R., Duggal, G., Love, M. I., Irizarry, R. A., and Kingsford, C.: Salmon provides fast and bias-aware quantification of transcript expression, Nat. Methods., 14, 417–419, 2017.

R Development Core Team: R: a language and environment for statistical computing, v. 4.0.3. [WWW document] URL www.r-project.org [accessed 10 October 2020].

Smith-Unna, R., Boursnell, C., Patro, R., Hibberd, J. M. and Kelly, S.: TransRate: Reference-free quality assessment of *de novo* transcriptome assemblies, Genome Res., 26, 1134–1144, 2016.

Wickham, H.: ggplot2: elegant graphics for data analysis, R package v.3.3.2. [WWW document] URL. https://cran.r-project.org/web/packages/ggplot2/index.html [accessed 17 June 2020], 2016.

Wingett, S. W and Andrews, S.: FASTQ screen: a tool for multi-genome mapping and quality control, F1000Research, 7, 1338, 2018.

Zhang, Y., Li, Z. K., Schulz, K. G., Hu, Y., Irwin, A. J., and Finkel, Z. V.: Growth-dependent changes in elemental stoichiometry and macromolecular allocation in the coccolithophore *Emiliania huxleyi* under different environmental conditions, Limnol. Oceanogr., 66, 2999–3009, doi: 10.1002/lno.11854, 2021.